



**TECHNISCHE
UNIVERSITÄT
WIEN**

Vienna University of Technology

DIPLOMARBEIT

**Solving singular BVPs in ODEs using
the MATLAB Code `bvpsuite`**

Ausgeführt am Institut für
Analysis and Scientific Computing
der Technischen Universität Wien

unter der Anleitung von
Ao. Univ. Prof. Dr. Ewa B. Weinmüller
Univ. Doz. Dr. Othmar Koch

durch Stefan Schirnhofner, BSc.
Rotenhofgasse 17 / 16
Vienna

October 20, 2015

Contents

1	Introduction	2
1.1	Boundary value problems with singular points	3
1.2	Analytical background	5
1.2.1	Stable and isolated solutions	5
1.2.2	Approximation problems	10
1.3	The MATLAB code <code>bvpsuite</code>	16
1.3.1	The collocation method	16
1.3.2	Basic solver in the MATLAB code <code>bvpsuite</code>	17
1.3.3	Estimate for the global error of the collocation solution	17
1.3.4	Mesh adaptation	18
1.3.5	Pathfollowing for parameter dependent problems	19
2	Computational Approaches to Singular Free Boundary Problems in Ordinary Differential Equations	20
2.1	Introduction	20
2.2	Variable Substitution	21
2.3	Numerical Examples	22
2.3.1	Numerical Example 1	22
2.3.2	Numerical Example 2	24
2.3.3	Numerical Example 3	28
2.3.4	Numerical Example 4	33
2.3.5	Summary of Numerical Results	37
2.4	Conclusions	38
3	Solving the generalized Korteweg-de Vries equation with <code>bvpsuite</code>	39
3.1	Introduction	39
3.2	Problem setting ($p \geq 6$)	40
3.2.1	Convergence orders and plots of numerical solutions for $p = 6$	41
3.3	Solution plots for different values of p	44
3.4	Solving the problem for $p = 6$ with adaptive mesh option	46
3.5	Time evolution of $u(x, t)$	47
3.6	Reduction of p from $p = 6$ to $p = 5$	49
3.7	Comparing the self-similar and homoclinic solutions.	52
3.8	Problem Setting ($p = 5$)	57
3.8.1	Convergence orders and plots of numerical solutions for $p = 5$	58
3.8.2	Solution plots for different values of q	60
3.9	Conclusions	61

Abstract

This master thesis deals with the solution of boundary value problems using the MATLAB code `bvpsuite` developed at the institute for Analysis and Scientific Computing of the Vienna University of Technology. Motivated by an international cooperation with P.M. Lima from the University of Lisbon and M.L. Morgado from the University of Trás-os-Montes e Alto Douro, Portugal, we are concerned with a singular free boundary problem for a second order nonlinear ordinary differential equation, where the differential operator is the degenerate m -Laplacian. The aim is to find a real $M > 0$ and a positive solution of the equation

$$(|y'|^{m-2} y')' + \frac{N-1}{x} |y'|^{m-2} y' + f(y) = 0, \quad 0 < x < M,$$

which belongs to $C^2((0, M)) \cap C^1([0, M])$ and satisfies the boundary conditions

$$y'(0) = 0, \quad y(M) = y'(M) = 0, \quad M > 0.$$

In [42], a numerical method has been proposed to approximate the solution of the above free boundary problem, where smoothing variable transformations are applied to deal with the singularities at $x = 0$ and $x = M$. The problem was discretized by means of a finite difference scheme.

In Section 2, we consider a new numerical approach. First we transform the free boundary problem into a boundary value problem on a fixed interval featuring an unknown constant λ . By applying to the resulting equations smoothing variable transformations, described in [42], we obtain a new problem, which we solve using the open domain MATLAB code `bvpsuite` [36].

Another cooperation with C. Budd from the University of Bath, United Kingdom, deals with the analysis of a self-similar blow-up solution of the generalized Korteweg-de Vries equation, computed in [20], which satisfies the following third order nonlinear ordinary differential equation, subject to boundary conditions:

$$\begin{aligned} \frac{2}{3(p-1)} w + \frac{\xi}{3} w_\xi + (w_{\xi\xi} + w^p)_\xi &= 0, \quad \xi \in \mathbb{R}, \\ \frac{2}{3(p-1)} w(\xi) + \frac{\xi}{3} w_\xi(\xi) &\xrightarrow{\xi \rightarrow \pm\infty} 0, \quad w_{\xi\xi}(\xi) \xrightarrow{\xi \rightarrow \infty} 0. \end{aligned}$$

This problem is posed on the infinite interval $(-\infty, \infty)$. The structure of the self-similar solution $\omega(\xi)$ is numerically studied with the MATLAB code `bvpsuite` by reducing ξ to a finite interval $[-L, L]$. The behaviour near the peak of the solution is analyzed, by decreasing p to 5 and comparing it to the homoclinic solution of a related second order linear ordinary differential equation. An asymptotic theory, which is under development, predicts that the self-similar solution becomes oscillatory and blows-up in the H^1 norm. The derivative of the self-similar solution - necessary for the calculation of the H^1 norm - is approximated by a sum of at most eight Gaussian functions. Further results, supporting an emerging asymptotic theory as $p \rightarrow 5$, can be found in Section 3.

1 Introduction

In this section, we first consider the state of the art on boundary value problems (BVPs) in ordinary differential equations (ODEs) and then briefly call in mind the classical analytical results describing the convergence properties of numerical schemes applied to solve BVPs in ODEs [32, 33]. Finally, the open domain MATLAB code `bvpsuite` [36] including not only the algorithm providing the numerical approximation to the solution of the analytical problem but also all necessary controlling mechanisms, error estimation procedure and grid adaptation strategy implemented in order to enhance the efficiency of the code is described.

This section is closely aligned with Section 1 of [55], where the analytical background about approximation methods for nonlinear problems and the code `bvpsuite` are also introduced.

In this thesis we focus on ODEs, but in more general situations, such models can take the form of partial differential equations or differential-algebraic equations (DAEs). ODEs play a fundamental role in technology and the natural sciences, since many technical processes and natural laws can be modelled by them. All these equations are subject to boundary condition (BCs) and/or initial conditions (ICs) prescribed to guarantee that the solution of the analytical problem is unique, or at least locally unique.

The next step towards a numerical solution consists of providing a suitable numerical method approximating the analytical solution in a reasonable way which means that with growing effort put into the numerical approximation its accuracy improves. In this work, we deal with the so-called discretization methods. This means that on the interval of integration a grid with a stepsize h is introduced and on this grid the values of the approximation are computed. Alternatively, we can also try to approximate the unknown solution by analytical functions, piecewise polynomials, for instance. Clearly, providing to the user an approximation without any information on its accuracy is not very helpful. Usually, the user will expect that the approximation satisfies the prescribed absolute and relative tolerance requirement, which can be roughly of the form

$$\| \text{error} \| \leq TOL_a + TOL_r \| \text{exact solution} \|,$$

where TOL_a , TOL_r are the absolute and relative tolerances, respectively. Clearly, it would be very advantageous to provide a numerical solutions satisfying the above requirement with possibly the least amount of work (on a grid with the least number of grid points). To this aim, since the exact error is not known, we need an *error estimate* correctly reflecting the size of the true error. Moreover, it turns out that working on *nonequidistant grids* is very often more advantageous, especially in cases when the solution behavior is different in different regions of the integration interval, see Subsection 1.3. In practice, the above error control is replaced by the executable requirement

$$\| \text{error estimate} \| \leq TOL_a + TOL_r \| \text{approximate solution} \|.$$

1.1 Boundary value problems with singular points

In recent years, scientific work carried out at the Institute for Analysis and Scientific Computing, Vienna University of Technology, included the analysis and numerical treatment of BVPs in ODEs which can exhibit singularities. Such problems often have the following form:

$$z'(t) = \frac{1}{t^\alpha} M(t)z(t) + f(t, z(t)), \quad t \in (0, 1], \quad (1)$$

$$b(z(0), z(1)) = 0, \quad (2)$$

$$z \in C[0, 1] \cap C^1(0, 1], \quad (3)$$

where $\alpha \geq 1$, z is an n -dimensional real function, M is a smooth $n \times n$ matrix, and $f \in \mathbb{R}^n$, $b \in \mathbb{R}^m$ are smooth functions. For $\alpha = 1$ the problem is called singular with a singularity of the first kind, for $\alpha > 1$ it is essentially singular (singularity of the second kind). In general, $m < n$ holds and condition (3) is equivalent to $n - m$ linearly independent conditions $z(0)$ must satisfy. These boundary conditions, augmented by (2), are necessary for the solution z to be isolated and for the problem (1) to be well-posed. In particular, problems posed on infinite intervals are frequently transformed to this problem class, with $\alpha > 1$.

The search for efficient numerical methods to solve (1)–(3) is strongly motivated by numerous applications from physics [16, 17, 31, 60] chemistry [22, 50, 56], mechanics [21], ecology [37, 43], or economy [25, 27, 30]. Also, research activities in related fields, like the computation of connecting orbits in dynamical systems [45], differential algebraic equations [47] or singular Sturm-Liouville problems [?], benefit from techniques developed for problems of the form (1)–(3).

Motivated by the above applications, a sound theoretical basis and the implementation of an open domain MATLAB code `sbvp` for the numerical solution of BVPs with a singularity of the first kind, $\alpha = 1$, have been provided. To compute the numerical solution of (1), polynomial collocation, with the collocation points placed in the interior of a collocation interval, was proposed [29, 57]. The decision to use collocation was motivated by its advantageous convergence properties for (1). For problems with smooth solutions, the convergence order is at least equal to the so-called *stage order* of the method. For the collocation schemes (at equidistant inner points or Gaussian points) this convergence results mean that a collocation scheme with s inner collocation points constitutes a high order basic solver ($O(h^s)$ uniformly in t), robust with respect to the singularity of the first kind. Here, we denoted by h the maximal stepsize in a nonequidistant grid.

In order to solve the ODE systems efficiently the meshes have to be adapted to the solution behavior. For singular problems, it is important to obtain meshes which are not affected by the steep direction field, staying coarse also close to the singularity when the solution

is smooth in that region. To design a mesh adaptation procedure, we need an efficient asymptotically correct a posteriori estimate for the error of the numerical solution. We control the global error because in the context of singular problems, the values of the residual (a local error measure) are as a rule orders of magnitude larger than the global error. Thus, it often turns out that grids generated via the equidistribution of the residual are too fine and generate solutions whose global errors are dramatically smaller than the prescribed tolerance, which is inefficient. The global error estimate was introduced in [5] and is based on the defect correction principle. It could be shown that for a collocation method of order $O(h^s)$, the error of the estimate (the difference between the exact global error and its estimate) is of order $O(h^{s+1})$, see [8, 38]. This asymptotically correct error estimate yields a reliable basis for an efficient mesh selection procedure. The respective grid adaptation procedure results in grids which adequately reflect the solution behavior. Experimental evidence showing that the procedure works efficiently and dependably for singular problems can be found in [5], and a theoretical justification is given in [9].

In the final step an open domain MATLAB code for explicit first order singular problems including an error estimation routine and a grid selection strategy was implemented. This code, `sbvp1.0` for MATLAB 6.0, has been published in 2002, and is available from

<http://www.mathworks.com/matlabcentral/fileexchange> >
 Mathematics >
 Differential Equations > SBVP1.0 Package.

Comprehensive information on the program and its performance can be found in [6, 5].

Due to the robustness of collocation, this method was used in one of the best established standard FORTRAN codes for (regular) BVPs, COLNEW, see [2, 3], and in `bvp4c`, the standard MATLAB module for (regular) ODEs with an option for singular problems, cf. [53]. In the scope of the FORTRAN code COLNEW are *explicit* systems of at most order four with multi-point boundary conditions. The code is using the $h-h/2$ strategy for the error estimation which means that the expensive collocation method is carried out twice, on the original mesh and on the refined mesh with the doubled number of mesh points. The Matlab code `bvp4c` solves also *explicit* ODE systems and is based on Lobatto collocation. As already mentioned, the control of the defect used in this code is especially disadvantageous for singular problems compared to controlling the global error in `sbvp`. Therefore, the meshes provided by `bvp4c` become unnecessarily dense. Comparing `sbvp` with COLNEW and `bvp4c` indicates a very satisfactory performance of the code. It is competitive with COLNEW and for the above reasons strongly superior to `bvp4c`. For details see [7].

Nevertheless, a further development of `sbvp` was necessary and resulted in a new code `bvpsuite` which will be described in more detail in Subsection 1.3. The scope of this new code is much wider than that of COLNEW, `bvp4c`, and the BVP SOLVER [54] and includes, among others, fully implicit ODE systems with multi-point boundary conditions, arbitrary degree of the differential equations including zero, module for dealing

with infinite intervals, a module for eigenvalue problems, free parameters, and a path-following strategy for parameter-dependent problems with turning points [36].

1.2 Analytical background

Here, we recapitulate the analytical results provided in [32]. We study nonlinear operator equations of the form

$$F(x) = 0, \quad F : B_1 \rightarrow B_2, \quad (4)$$

where B_1, B_2 are suitably defined Banach spaces. A Banach space is complete, which means that all Cauchy series converge in the underlying norm. We first introduce two important properties of solutions of (4), stable and isolated solutions. We will also deal with properties of the discrete problem class related to (4),

$$F_h(x_h) = 0, \quad F : B_1^h \rightarrow B_2^h,$$

where B_1^h, B_2^h are appropriately defined finite dimensional Banach spaces.

1.2.1 Stable and isolated solutions

Here, we discuss in more detail the stable and isolated solutions of (4), especially the question how these two attributes are related to each other. We stress, that we do not aim at showing the existence of solutions to (4). A solution *is assumed* to exist. From the numerical point of view the *stability* and the *isolatedness of the solution* are the key issues. As we will see these two properties are closely related.

We note that stability will be a crucial property for the convergence of the scheme, also in context of numerical schemes and for the Newton method, used to solve the involved nonlinear system of algebraic equations.

Let $u \in B_1$ be a solution of $F(x) = 0$ and let us introduce the sphere $S_\rho(u)$ defined by

$$S_\rho(u) := \{x \mid x \in B_1, \|x - u\| \leq \rho\}.$$

In the following, when it cannot be misleading, we use the abbreviation $S_\rho := S_\rho(u)$.

Definition 1. *The mapping $F(\cdot)$ is stable on S_ρ , iff there exists a constant $K_\rho > 0$ such that*

$$\|w - v\| \leq K_\rho \|F(w) - F(v)\|$$

for all $w, v \in S_\rho$.

Definition 2 (Stable solution). *A solution u of (4) is stable, iff $F(\cdot)$ is stable on S_ρ for some $\rho > 0$.*

Lemma 1. *A stable solution is unique in S_ρ (locally unique).*

Proof. Let u_1 and u_2 be two different stable solutions of (4). This means that

$$F(u_1) = F(u_2) = 0.$$

Since u_1 and u_2 are stable, F is stable and therefore,

$$\|u_1 - u_2\| \leq K_\rho \|F(u_1) - F(u_2)\| = 0.$$

This implies that u is unique. □

Another important notion in this context is an *isolated solution*. In the following, we denote the Fréchet derivative of F at point x by $L(x)$. The operator $L(x)$ is a linear bounded operator, $L(x) : B_1 \rightarrow B_2$, such that

$$r(x, y) = \frac{\|F(x + y) - [F(x) + L(x)y]\|}{\|y\|} \rightarrow 0 \text{ as } \|y\| \rightarrow 0. \quad (5)$$

The definition of an isolated solution can now be introduced.

Definition 3 (Isolated solution). *A solution u of (4) is isolated, iff $L(u)$ exists and is nonsingular; that is*

$$L(u)y = 0 \Leftrightarrow y = 0,$$

where $L(u) : B_1 \rightarrow B_2$.

The above condition means that $L(u)$ is injective. From now on we assume that B_1 is the domain of $L(u)$, and that $L(u)$ maps B_1 onto B_2 . This means that the range of $L(u)$, $\mathcal{R}(L(u)) = B_2$. Consequently, this implies that

$$L(u) : \mathcal{D}(L(u)) = B_1 \rightarrow \mathcal{R}(L(u)) = B_2$$

is bijective and $L^{-1}(u) : B_2 \rightarrow B_1$ exists.

For below Theorem 2, we need more than that. In the proof, we use that $L(u)$ has a *bounded inverse*. If for the operator $L(u)$ specified above, we additionally assume that $L(u)$ is bounded, then it follows from the *Open Mapping Theorem* that $L^{-1}(u)$ is bounded.

Remark 1. *The notion nonsingular is ‘borrowed’ from linear algebra. Let us consider the linear system of equations*

$$Ay = 0, \quad A \in \mathbb{R}^{n \times n}.$$

Then the matrix A is nonsingular iff

$$Ay = 0 \Leftrightarrow y = 0.$$

Here, we have a finite dimensional situation and therefore, if A is nonsingular, A is bijective, and consequently, A^{-1} exists. Equivalently, for any $b \in \mathbb{R}^n$ there exists a unique $x \in \mathbb{R}^n$, such that $Ax = b$.

We now investigate how these two important properties of the solutions of (4) are related. We first show that *stability implies isolatedness*.

Theorem 1. *Let u be a stable solution of (4). Then, if $L(u)$ exists, it is nonsingular, and consequently, u is isolated.*

Proof. The proof is indirect. We assume that $L(u)y = 0$ but $\|y\| \neq 0$. In this case, for all positive scalars $a < \rho/\|y\|$ it follows that $v(a) = u + ay \in S_\rho$.

The fact that $F(\cdot)$ is stable on S_ρ yields

$$\|u - v(a)\| \leq K_\rho \|F(u) - F(v(a))\|.$$

We now set $x := u$ and $y := ay$ in $r(x, y)$, and obtain

$$r(u, ay) = \frac{\|F(v) - [F(u) + L(u)ay]\|}{\|ay\|}$$

and therefore,

$$r(u, ay)\|ay\| = \|(F(v) - F(u)) - L(u)ay\|.$$

From the triangle inequality,

$$r(u, ay)\|ay\| + \|L(u)ay\| \geq \|(F(v) - F(u))\|,$$

and we conclude that

$$\|u - v(a)\| \leq K_\rho \{r(u, ay)\|ay\| + \|L(u)ay\|\}.$$

This is equivalent to

$$a\|y\| \leq K_\rho r(u, ay)a\|y\|.$$

If we choose $a > 0$, so small that $K_\rho r(u, ay) < 1$, then $\|y\| = 0$ holds which contradicts the assumption. \square

Stability is such a strong condition that it implies that $L(x)$ is nonsingular wherever it exists in the *interior* of $S_\rho(u)$.

This result suggests a further question: Let u be isolated. Does this imply that u is stable? The next theorem shows, that in this case we need an additional assumption on $L(x)$, its Lipschitz continuity w.r.t. x .

Theorem 2. *Let us make the following assumptions:*

- (a) $L(u)$ is nonsingular and has a bounded inverse for some $u \in B_1$.

(b) Let $L(x)$ exist and be Lipschitz continuous on $S_{\rho_0}(u)$ for some ρ_0 . This means that for some constant $K_L > 0$, $\|L(x) - L(y)\| \leq K_L\|x - y\|$ for all $x, y \in S_{\rho_0}$.

Then, $F(\cdot)$ is stable on S_ρ for $\rho < (K_L\|L^{-1}(u)\|)^{-1}$ and the stability constant is

$$K_\rho = \|L^{-1}(u)\|(1 - \rho K_L\|L^{-1}(u)\|)^{-1}.$$

Proof. We want to show that under the above assumptions, there exists a constant $K_\rho > 0$ such that

$$\|x - y\| \leq K_\rho\|F(x) - F(y)\|$$

for all $x, y \in S_\rho$. From the generalized *Mean Value Theorem*, we see that for any $x, y \in S_\rho$ with $\rho \leq \rho_0$,

$$F(x) - F(y) = \tilde{L}(x, y)(x - y),$$

where

$$\tilde{L}(x, y) = \int_0^1 L(tx + (1 - t)y)dt.$$

Now, we show that $(\tilde{L}(x, y))^{-1}$ exists and that its norm, $\|\tilde{L}^{-1}(x, y)\|$, is bounded. Then, we immediately have

$$(\tilde{L}(x, y))^{-1}(F(x) - F(y)) = x - y \Rightarrow \|x - y\| \leq \underbrace{\|(\tilde{L}(x, y))^{-1}\|}_{K_\rho} \|F(x) - F(y)\|.$$

Let us write

$$\tilde{L}(x, y) = L(u) + [\tilde{L}(x, y) - L(u)]$$

and note that

$$\begin{aligned} \|\tilde{L}(x, y) - L(u)\| &\leq \int_0^1 \|L(tx + (1 - t)y) - L(tu + (1 - t)u)\|dt \\ &\leq K_L \int_0^1 \|t(x - u) + (1 - t)(y - u)\|dt \\ &\leq K_L\rho, \end{aligned} \tag{6}$$

where we used the fact that L is Lipschitz continuous. Now we use the so-called *Banach Lemma*, see [40], to find an upper bound for $\|\tilde{L}^{-1}(x, y)\|$.

Lemma 2 (Banach Lemma). *Let $A, C : B_1 \rightarrow B_2$, be two linear bounded operators, and B_1, B_2 two Banach spaces. Let A^{-1} exist and $\|A^{-1}C\| < 1$. Then, $(A - C)^{-1}$ exist and*

$$\|(A - C)^{-1}\| \leq \frac{\|A^{-1}\|}{1 - \|A^{-1}C\|}.$$

We apply this lemma in the following way: Let $A = L(u)$ and $C = -\tilde{L}(x, y) + L(u)$. If ρ is so small that $\rho K_L \|L^{-1}\| < 1$ holds, then the Banach Lemma implies that \tilde{L} is nonsingular and

$$\|\tilde{L}^{-1}(x, y)\| \leq \frac{\|L^{-1}(u)\|}{1 - \rho K_L \|L^{-1}(u)\|}.$$

This means that $F(\cdot)$ is stable and the norm of \tilde{L}^{-1} is the stability constant of F . This completes the proof.

We summarize: If u is an isolated solution of (4) and $L(u)^{-1}$ exists, then it is nonsingular. In addition, if $L(x)$ exists and is Lipschitz continuous in some $S_{\rho_0}(u)$, then u is stable. \square

Remark 2. *It follows from the above considerations that stable problems are well-posed. By definition, the problem $F(x) = 0$ is well-posed, when a unique solution u exists. Moreover, if each of the problems $F(x_i) = f_i$ has a solution, then*

$$\lim_{\|f_i\| \rightarrow 0} \|u - x_i\| = 0.$$

In other words, the solution is unique (at least locally) and it depends continuously on the problem data.

Remark 3. *We now try to interpret the result formulated in Theorem 2. Consider the system of nonlinear algebraic equations*

$$F(x) = 0, \quad F : \mathbb{R}^n \rightarrow \mathbb{R}^n.$$

Assume

- $L(u) = \frac{\partial F(u)}{\partial x}$ is nonsingular for the solution u .
- Let $L(x)$ be continuous on $U \subset \mathbb{R}^n$.

Then, there exist $S_{\rho_1}(u)$ and $S_{\rho_2}(0)$ such that there exists a continuous local inverse $F^{-1} : S_{\rho_2}(0) \rightarrow S_{\rho_1}(u)$, or equivalently, for each $g \in S_{\rho_2}(0)$ there exists a unique $x \in S_{\rho_1}(u)$ with $F(x) = g$. This is the theorem about the ‘local invertibility’. We know about this fact in the context of systems of nonlinear equations, but an analogous result holds for nonlinear operator equations.

The local invertibility is crucial for the convergence of the Newton method.

1.2.2 Approximation problems

This section is devoted to the properties of discretization schemes applied to solve the analytical problem.

For the family of Banach spaces B_1^h, B_2^h , we consider the family of approximating problems, for $0 < h \leq h_0$,

$$F_h(x_h) = 0, \quad (7)$$

where $F_h : B_1^h \rightarrow B_2^h$.

Example: We consider the following nonlinear scalar problem:

$$N(y) = \begin{cases} y'(t) - f(t, y(t)), & t \in [0, 1] \\ a_1 y(0) + a_2 y(1) - a_3, & \end{cases}, \quad (8)$$

where $y : [0, 1] \rightarrow \mathbb{R}$ and $f : [0, 1] \times \mathbb{R} \rightarrow \mathbb{R}$. A very simple example of a family of approximating problems is resulting from the so-called forward Euler rule.

Let us introduce a mesh on the interval $[0, 1]$,

$$\Delta_h := \{t_i \mid t_i = ih, i = 0, 1, \dots, N, h = t_{i+1} - t_i\}.$$

Then the discretization scheme takes the form

$$N_h(y_h) = \begin{cases} \frac{y_{i+1} - y_i}{h} - f(t_i, y_i) = 0, & i = 0, \dots, N-1, \\ a_1 y_0 + a_2 y_N - a_3 = 0, & \end{cases} \quad (9)$$

where $y_i \approx y(t_i)$ and $y_h = (y_0, y_1, \dots, y_N)^T$.

To relate the problems $F(x) = 0$ and $F_h(x_h) = 0$, we require that there exists a family of linear mappings P_1^h, P_2^h , such that

$$(a) P_\nu^h : B_\nu \rightarrow B_\nu^h, \quad (b) \lim_{h \rightarrow 0} \|P_\nu^h x\|_{B_\nu^h} = \|x\|_{B_\nu}, \quad \forall x \in B_\nu. \quad (10)$$

We use the notation from [32],

$$P_\nu^h x := [x]_h, \quad \nu = 1, 2,$$

where, $[x]_h \in B_\nu^h$ if $x \in B_\nu$. In our example above $[y]_h = (y(t_0), \dots, y(t_N))^T$. We now study the so-called global discretization error,

$$\|[y^*]_h - y_h\|$$

with appropriately chosen norm in B_1^h , where y^* is the exact solution of (8). Especially, we are interested in answering the question if and how fast the global error tends to zero for h tending to zero.

$$\lim_{h \rightarrow 0} \|[y^*]_h - y_h\| = O(h^p), \quad p > 0.$$

The Fréchet derivative of F_h at x_h is denoted by $L_h(x_h)$, where $S_\rho(x_h)$ is the sphere in B_1^h with radius ρ about x_h . As a next step we introduce the necessary concepts. In the following, we always assume that a stable (and therefore locally unique) solution $u \in B_1$ with $F(u) = 0$ exists.

Definition 4. *The family $\{F_h(\cdot)\}$ is stable for $u \in B_1$, iff for some $h_0 > 0$, $\rho > 0$ and some constant M_ρ , independently of h ,*

$$\|x_h - y_h\| \leq M_\rho \|F_h(x_h) - F_h(y_h)\|,$$

for all $x_h, y_h \in S_\rho([u]_h)$ and all $h \in (0, h_0]$.

Definition 5. *The family $\{F_h(\cdot)\}$ is consistent of order p with $F(\cdot)$ on $S_\rho(u)$, iff*

$$\|F_h([x]_h) - [F(x)]_h\| := \|\tau_h(x)\| \leq M(x)h^p$$

for all $x \in S_\rho(u)$ and some bounded functional $M(x) \geq 0$ independent of h .

We first interpret the last definition in the context of our example. What we need to look at is,

$$N_h([y]_h) - [N(y)]_h,$$

where

$$N_h([y]_h) = \begin{cases} \frac{y^{(t_{i+1})} - y^{(t_i)}}{h} - f(t_i, y^{(t_i)}), & i = 0, \dots, N-1, \\ a_1 y(t_0) + a_1 y(t_N) - a_3 = a_1 y(0) + a_1 y(1) - a_3, \end{cases}$$

and

$$[N(y)]_h = \begin{cases} y'(t_i) - f(t_i, y^{(t_i)}), & i = 0, \dots, N-1, \\ a_1 y(0) + a_1 y(1) - a_3, \end{cases}$$

which means

$$N_h([y]_h) - [N(y)]_h = \begin{cases} \frac{y^{(t_{i+1})} - y^{(t_i)}}{h} - y'(t_i), & i = 0, \dots, N-1, \\ 0. \end{cases}$$

Note that for the solution y^* , with $N(y^*) = 0$,

$$N_h([y^*]_h) - [N(y^*)]_h = \begin{cases} \frac{y^*(t_{i+1}) - y^*(t_i)}{h} - \underbrace{f(t_i, y^*(t_i))}_{(y^*)'(t_i)}, & i = 0, \dots, N-1, \\ 0. \end{cases}$$

The quantity $\tau_h(y^*) = N_h([y^*]_h) - [N(y^*)]_h = N_h([y^*]_h)$ is called *residual*, sometimes also *local discretization error*.

The significance of these definitions can be seen in the next theorem where we use stability to ‘sum up’ the *local errors* in order to obtain an a priori bound for the *global discretization error*.

Theorem 3. *Let $F(u) = 0$ and $F_h(v_h) = 0$ for some $v_h \in S_\rho([u]_h)$, $\rho > 0$ and all $h \in (0, h_0]$. Let $\{F_h(\cdot)\}$ be stable for u and consistent with $F(\cdot)$ of order p on $S_0(u)$. Then*

$$\|[u]_h - v_h\| \leq M_\rho M(u) h^p.$$

Proof. We set $x_h = [u]_h$ and $y_h = v_h$ and use the stability to obtain

$$\|[u]_h - v_h\| \leq M_\rho \|F_h([u]_h) - F_h(v_h)\|.$$

From $F_h(v_h) = 0$ and $[F(u)]_h = 0$, we have

$$\begin{aligned} \|[u]_h - v_h\| &\leq M_\rho \|F_h([u]_h) - F_h(v_h)\| = M_\rho \|F_h([u]_h) - [F(u)]_h\| \\ &\leq M_\rho M(u) h^p, \end{aligned}$$

and the result follows by consistency with $\rho = 0$. □

This theorem is often summarized by the famous

$$\text{Stability} + \text{Consistency} = \text{Convergence}.$$

For a particular scheme F_h , we still need to answer the following questions:

- Does the approximating problem $F_h(x_h) = 0$ have a solution in some sphere $S_\rho([u]_h)$?
- Can we verify stability?
- Can we determine the order of consistency?

The difficulty of these questions varies with the schemes we are considering. Stability of explicit difference schemes can be often easily verified, but it is hard to verify stability for implicit schemes. Often consistency can be investigated by a simple Taylor argument. In case of the forward Euler and $y \in C^2$, it immediately follows

$$N_h([y]_h) - [N(y)]_h = \frac{y(t_{i+1}) - y(t_i)}{h} - y'(t_i) = \frac{h}{2} y''(\eta_i), \quad i = 0, \dots, N-1,$$

with order of consistency $p = 1$. Because stability is very difficult to show, in general, it is useful to know under which circumstances this analysis can be restricted to the study of the linearized problems.

The aim of the next lemma is to formulate sufficient conditions for $\{F_h(\cdot)\}$ to be stable.

Theorem 4. *Let the family of mappings $\{F_h(\cdot)\}$ have Fréchet derivatives, i.e., linearizations, $\{L_h(x_h)\}$ on some family of spheres $S_{\rho_0}(z_h)$ and satisfy for all $h \in (0, h_0]$:*

- (a) $\{L_h(z_h)\}$ have uniformly bounded inverses at the centers of the spheres; that is, for some constant $K_0 > 0$, $\|L_h^{-1}(z_h)\| \leq K_0$.
- (b) $\{L_h(x_h)\}$ are uniformly Lipschitz continuous on $S_{\rho_0}(z_h)$; that is, for some constant $K_L > 0$,

$$\|L_h(x_h) - L_h(y_h)\| \leq K_L \|x_h - y_h\|$$

for all $x_h, y_h \in S_{\rho_0}(z_h)$.

If $z_h = [u]_h$ for some $u \in B_1$, then the family $\{F_h(\cdot)\}$ is stable for u .

The proof of Theorem 4 is essentially identical to the proof given in Theorem 2.

To ensure the existence of a family of solutions $\{v_h\}$ approximating a solution u , we need only to add consistency to the above. This is done in the next theorem.

Theorem 5. *Let $x = u$ be a solution of $F(x) = 0$. Let the family $\{F_h(\cdot)\}$ be consistent of order p with $F(\cdot)$ on $S_0(u)$. Let the hypotheses (a) and (b) from Theorem 4 hold with $z_h = [u]_h$. Then, for ρ_0 and h_0 sufficiently small and for each $h \in (0, h_0]$, the problem $F_h(x_h) = 0$ has a unique solution $x_h = v_h \in S_{\rho_0}([u]_h)$. The solutions v_h satisfy*

$$\|[u]_h - v_h\| \leq M_{\rho_0} M(u) h^p.$$

Proof. To show the result we use the *Banach Fixed Point Theorem*. Therefore, we define a family of mappings $\{G_h(x_h)\}$ by

$$G_h(x_h) := x_h - L_h^{-1}([u]_h) F_h(x_h)$$

and show that they are uniformly contracting on $S_{\rho_0}([u]_h)$, provided that ρ_0 and h_0 are sufficiently small. For any $x_h, y_h \in S_{\rho_0}([u]_h)$ we have

$$\begin{aligned} G_h(x_h) - G_h(y_h) &= x_h - y_h - L_h^{-1}([u]_h)(F_h(x_h) - F_h(y_h)) \\ &= L_h^{-1}([u]_h)\{L_h([u]_h)(x_h - y_h) - (F_h(x_h) - F_h(y_h))\} \\ &= L_h^{-1}([u]_h)\{L_h([u]_h) - \hat{L}_h(x_h, y_h)\}(x_h - y_h), \end{aligned}$$

where

$$\hat{L}_h(x_h, y_h) := \int_0^1 L_h(tx_h + (1-t)y_h) dt,$$

with $tx_h + (1-t)y_h \in S_{\rho_0}([u]_h)$, because $S_{\rho_0}([u]_h)$ is convex. From (b) in Theorem 4, it follows that

$$\|L_h([u]_h) - \hat{L}_h(x_h, y_h)\| \leq K_L \rho_0$$

and thus, from (a) in Theorem 4 we have

$$\|G_h(x_h) - G_h(y_h)\| \leq \alpha \|x_h - y_h\|, \quad \alpha = K_0 K_L \rho_0.$$

At the center of the sphere, $x_h = [u]_h$, we have, by consistency and since $F(u) = 0$,

$$\begin{aligned} G_h(x_h) &:= x_h - L_h^{-1}([u]_h)F_h(x_h) \Rightarrow G_h([u]_h) := [u]_h - L_h^{-1}([u]_h)F_h([u]_h) \Rightarrow \\ &\| [u]_h - G_h([u]_h) \| \leq \| L_h^{-1}([u]_h) \| \| F_h([u]_h) - [F(u)]_h \| \leq K_0 M(u) h^p. \end{aligned}$$

If $\alpha < 1$ and $K_0 M(u) h^p \leq (1 - \alpha) \rho_0$, the Banach Fixed Point Theorem (*Contraction Mapping Theorem*) applied to $x_h = G(x_h)$ implies the existence of a unique solution in $S_{\rho_0}([u]_h)$. The error estimate from Theorem 3 is now applicable. \square

Clearly, since we do not know $[u]_h$ we cannot carry out the Newton iteration in a way discussed in the last theorem. Our final result deals with the convergence of the Newton method applied to solve $F_h(v_h) = 0$ on $S_{\rho_0}([u]_h)$.

Theorem 6. *Let the hypotheses of Theorem 5 hold. Then, for any $h \in (0, h_0]$, if ρ_0, h_0 and $\rho_1 \leq \rho_0$ are sufficiently small, the Newton iterates $\{v_h^{(\nu)}\}$ defined by*

- (a) $v_h^{(0)} \in S_{\rho_1}([u]_h)$,
- (b) $L_h(v_h^{(\nu)}) \left(v_h^{(\nu+1)} - v_h^{(\nu)} \right) = -F_h(v_h^{(\nu)})$, $\nu = 0, 1, \dots$,

converge quadratically to the solution v_h^* of $F_h(x_h) = 0$, $x_h \in S_{\rho_0}([u]_h)$.

Proof. We write

$$\begin{aligned} L_h(x_h) &= L_h([u]_h) + [L_h(x_h) - L_h([u]_h)] \\ &= L_h([u]_h) \left(I + \underbrace{(L_h([u]_h))^{-1} [L_h(x_h) - L_h([u]_h)]}_{=: -B} \right). \end{aligned}$$

From Theorem 4 (a) and (b), we have

$$\begin{aligned} \|B\| &= \|(L_h([u]_h))^{-1} [L_h(x_h) - L_h([u]_h)]\| \leq \\ &\underbrace{\|(L_h([u]_h))^{-1}\|}_{\leq K_0} \underbrace{\|[L_h(x_h) - L_h([u]_h)]\|}_{\leq K_L \rho_0}. \end{aligned}$$

For sufficiently small ρ_0 , $K_0 K_L \rho_0 < 1$. Thus, the inverse of $I - B$ exists by the Banach Lemma, and consequently, also the inverse of $L_h(x_h)$. Moreover,

$$\|(L_h(x_h))^{-1}\| \leq \underbrace{\|(I - B)^{-1}\|}_{\leq \frac{1}{1 - \|B\|}} \underbrace{\|(L_h([u]_h))^{-1}\|}_{\leq K_0} \leq \frac{K_0}{1 - K_0 K_L \rho_0} =: K_{\rho_0}, \quad (11)$$

for all $x_h \in S_{\rho_0}([u]_h)$.

This is really important: We would like to stress at this point that $(L_h(x_h))^{-1}$ exists for all $x_h \in S_{\rho_0}([u]_h)$ and not only for the center $[u]_h$ of $S_{\rho_0}([u]_h)$, as it was assumed in Theorem 4 (a).

Now, from (b) and $\nu = 0$, we calculate $v_h^{(1)} - v_h^{(0)}$,

$$\begin{aligned} v_h^{(1)} - v_h^{(0)} &= -(L_h(v_h^{(0)}))^{-1} F_h(v_h^{(0)}) \\ &= -(L_h(v_h^{(0)}))^{-1} (F_h(v_h^{(0)}) - F_h([u]_h) + F_h([u]_h)) \\ &= -(L_h(v_h^{(0)}))^{-1} F_h([u]_h) + (L_h(v_h^{(0)}))^{-1} (F_h([u]_h) - F_h(v_h^{(0)})) \\ &= -(L_h(v_h^{(0)}))^{-1} F_h([u]_h) + \underbrace{(L_h(v_h^{(0)}))^{-1} \widehat{L}_h([u]_h, v_h^{(0)})}_{=: D} ([u]_h - v_h^{(0)}). \end{aligned}$$

We first rewrite D ,

$$D = (L_h(v_h^{(0)}))^{-1} \widehat{L}_h([u]_h, v_h^{(0)}) = I + (L_h(v_h^{(0)}))^{-1} (\widehat{L}_h([u]_h, v_h^{(0)}) - L_h(v_h^{(0)})),$$

and have

$$\|D\| \leq 1 + \underbrace{\|(L_h(v_h^{(0)}))^{-1}\|}_{\leq C_1, \text{ see (11)}} \underbrace{\|\widehat{L}_h([u]_h, v_h^{(0)}) - L_h(v_h^{(0)})\|}_{\leq C_2} \leq C.$$

Consequently,

$$\begin{aligned} \|v_h^{(1)} - v_h^{(0)}\| &\leq \|(L_h(v_h^{(0)}))^{-1}\| \|F_h([u]_h)\| + \|D\| \|([u]_h - v_h^{(0)})\| \\ &= \|(L_h(v_h^{(0)}))^{-1}\| \|F_h([u]_h) - [F(u)]_h\| + \|D\| \|([u]_h - v_h^{(0)})\| \\ &\leq K_{\rho_0} M(u) h^p + C \rho_1. \end{aligned}$$

Clearly,

$$\|v_h^{(1)} - v_h^{(0)}\| \leq \rho_0 \tag{12}$$

provided that $h \leq h_0$ and $\rho_1 \leq \rho_0$ are sufficiently small. Remark: conditions (11)–(12) and Theorem 4 (b) are sufficient for the quadratic convergence of the Newton method on $S_{\rho_0}([u]_h)$, see [48]. \square

Let us summarize: If the nonlinear problem $F(x) = 0$ has an isolated solution u , the family of approximations $\{F_h(\cdot)\}$ is stable for u and consistent of order p with $F(\cdot) = 0$ on $S_{\rho_0}([u]_h)$, then there exists a stepsize h_0 such that for all $h \leq h_0$ the approximating problems $F_h(x_h) = 0$ have solutions v_h in $S_{\rho_0}([u]_h)$, provided ρ_0 is sufficiently small. For $h \rightarrow 0$ these solutions v_h converge to $[u]_h$ and the global error is of order p , $\|v_h - [u]_h\| = O(h^p)$. Moreover, there exists a constant $\rho_1 \leq \rho_0$ such that the Newton iteration converges quadratically in $S_{\rho_0}([u]_h)$ from any starting value $v_h^{(0)} \in S_{\rho_1}([u]_h)$, provided ρ_1 is sufficiently small.

1.3 The MATLAB code `bvpsuite`

Since the first version of the software, the code `sbvp`, did not cover many important applications, a new MATLAB code `bvpsuite` was developed to cope with fully implicit problems of mixed orders, parameter dependent problems, problems with unknown parameters, problems posed on semi-infinite intervals, eigenvalue problems and differential algebraic equations of index 1.

1.3.1 The collocation method

Since in `bvpsuite` polynomial collocation is used as the basic solver, we describe here the convergence of the method in the context of singular ODEs. We first define a mesh

$$\Delta := (\tau_0, \tau_1, \dots, \tau_N), \quad (13)$$

such that

$$h_i := \tau_{i+1} - \tau_i, \quad J_i := [\tau_i, \tau_{i+1}], \quad i = 0, \dots, N-1, \quad \tau_0 = 0, \quad \tau_N = 1, \quad (14)$$

see Figure 1.

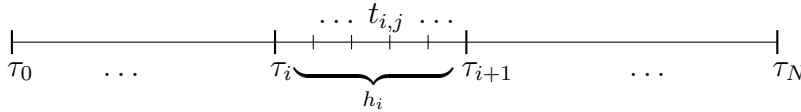


Figure 1: The computational grid

For the collocation, s points $t_{i,j}$, $j = 1, \dots, s$, are inserted in each subinterval J_i ,

$$t_{i,j} = \tau_i + \rho_j h_i, \quad j = 1, \dots, s, \quad 0 < \rho_1 < \rho_2 < \dots < \rho_s < 1. \quad (15)$$

Let us denote by \mathbb{P}_s the Banach space of continuous, piecewise polynomial functions p such that $p(t) := P_i(t)$, $t \in J_i$, $i = 0, \dots, N-1$, where P_i is a polynomial of degree $\leq s$. Consider the problem

$$z'(t) = \frac{M(t)}{t} z(t) + f(t, z(t)), \quad (16)$$

$$B(z(0), z(1)) = 0, \quad (17)$$

where $B : \mathbb{R}^n \times \mathbb{R}^n \rightarrow \mathbb{R}^n$, such that it is well-posed and has a locally unique solution z . Then, the approximation $p \in \mathbb{P}_s$ for z has to satisfy the so-called collocation conditions (18), $i = 0, \dots, N-1$, $j = 1, \dots, s$, and the boundary conditions (19),

$$p'(t_{i,j}) = \frac{M(t_{i,j})}{t_{i,j}} p(t_{i,j}) + f(t_{i,j}, p(t_{i,j})), \quad (18)$$

$$B(p(0), p(1)) = 0. \quad (19)$$

In [38] the convergence of the above schemes was studied. For problems with a singularity of the first kind, $\alpha = 1$, and appropriately smooth solutions, the scheme was shown to be uniquely solvable and to converge with order s up to possible logarithmic terms, uniformly in t ,

$$\|p - z\|_\infty := \max_{t \in [0,1]} |p(t) - z(t)| = O(h^s |\ln h|^k), \quad h \rightarrow 0,$$

where $k \in \mathbb{N}_0$. For further information we refer to [36, 6, 38].

1.3.2 Basic solver in the MATLAB code `bvpsuite`

The code is designed to solve systems of differential equations of arbitrary mixed order including zero¹, subject to initial or boundary conditions,

$$F(t, p_1, \dots, p_s, z_1(t), z_1'(t), \dots, z_1^{(l_1)}(t), \dots, z_n(t), z_n'(t), \dots, z_n^{(l_n)}(t)) = 0, \quad (20)$$

$$\begin{aligned} B(p_1, \dots, p_s, z_1(c_1), \dots, z_1^{(l_1-1)}(c_1), \dots, z_n(c_1), \dots, z_n^{(l_n-1)}(c_1), \dots, \\ z_1(c_q), \dots, z_1^{(l_1-1)}(c_q), \dots, z_n(c_q), \dots, z_n^{(l_n-1)}(c_q)) = 0, \end{aligned} \quad (21)$$

where the solution vector $z(t) = (z_1(t), z_2(t), \dots, z_n(t))^T$, and the parameters p_i , $i = 1, \dots, s$, are unknown. In general, $t \in [a, b]$ or $t \in [a, \infty)$, $a \geq 0$. Moreover,

$$F : [a, b] \times \mathbb{R}^s \times \mathbb{R}^{l_1} \times \dots \times \mathbb{R}^{l_n} \rightarrow \mathbb{R}^n$$

and

$$B : \mathbb{R}^s \times \mathbb{R}^{q_{l_1}} \times \dots \times \mathbb{R}^{q_{l_n}} \rightarrow \mathbb{R}^{l+s},$$

where $l := \sum_{i=1}^n l_i$. Note that boundary conditions can be posed on any subset of distinct points $c_i \in [a, b]$, $a \leq c_1 < c_2 < \dots < c_q \leq b$. For the numerical treatment, we assume that the BVP (20)–(21) is well-posed and has a locally unique solution z .

In order to find a numerical solution of (20)–(21) we introduce a mesh (13), partitioning the interval $[a, b]$ as shown in Figure 1 and apply polynomial collocation as described above. For details see [36]. We represent the collocation polynomials using the Runge-Kutta basis [4, 12]. The resulting nonlinear system for the coefficients of this representation is solved by the Newton method.

1.3.3 Estimate for the global error of the collocation solution

The estimate for the global error of the collocation solution is based on mesh halving. Let us assume that the numerical solution $p_\Delta(t)$ has been obtained using the mesh Δ with N

¹This means that differential algebraic equations are also in the scope of the code.

subintervals J_i of the length h_i . We now construct a second mesh Δ_2 where we replace every subinterval J_i by two subintervals of length $h_i/2$. On this new mesh the collocation solution $p_{\Delta_2}(t)$ is computed. We use these two collocation solutions to define the error estimate for the approximation $p_{\Delta}(t)$,

$$\mathcal{E}(t) := \frac{2^s}{1 - 2^s} (p_{\Delta_2}(t) - p_{\Delta}(t)), \quad t \in J_i.$$

In case that the global error $\delta(t) := p_{\Delta}(t) - z(t)$ of the collocation solution from the coarse mesh can be expressed in terms of the principal error function $e(t)$,

$$\delta(t) = e(t)h_i^s + O(h_i^{s+1}), \quad t \in J_i,$$

where $e(t)$ is independent of Δ , the above error estimate is asymptotically correct, since $\mathcal{E}(t)$ satisfies

$$\mathcal{E}(t) - \delta(t) = O(h^{s+1}),$$

where $h = \max_{1 \leq i \leq N} h_i$. The above estimate for the global error works well for both, problems with a singularity of the first and of the second kind [6, 52, 23]. This method is applicable for problems in explicit and implicit form (therefore, also for DAEs) without modifications [36].

1.3.4 Mesh adaptation

In general, by uniformly decreasing the stepsize h it will be possible to satisfy the given tolerance requirement but this strategy is inefficient because it does not take into account the solution behavior and the structure of the error. Therefore, the appropriate mesh adaptation is a reasonable measure for saving time and effort. The mesh selection strategy implemented in `bvpsuite` was proposed and investigated in [49]. A correct error estimate of the global error is a good indicator for the regions where the solution is difficult to approximate. These regions usually show a rapid solution (or higher derivatives) change. The main idea of the mesh adaptation is to locate the grid points in such a way that the global error becomes equidistributed or constant along the grid. This means that the stepsize has to become smaller in the regions where the solution is difficult and larger where it is smooth.

Grid adaptation in two-point boundary value problems is usually based on mapping a uniform auxiliary grid to the desired nonuniform grid. In `bvpsuite` this approach is combined with a new control system for constructing a grid density function $\phi(\tau)$. The local mesh width $\Delta\tau_{i+1/2} = \tau_{i+1} - \tau_i$ with $0 = \tau_0 < \tau_1 < \dots < \tau_N = 1$ is computed as $\Delta\tau_{i+1/2} = \frac{\epsilon_N}{\varphi_{i+1/2}}$, where $\{\varphi_{i+1/2}\}_0^{N-1}$ is a discrete approximation to the continuous density function $\phi(\tau)$, representing mesh width variation. The parameter $\epsilon_N = 1/N$ controls accuracy via the choice of N . For any given grid, a solver provides an error estimate on a coarse control grid. Taking this as its input, the feedback control law then adjusts the

grid, and the interaction continues until the monitor function (in this case the residual) has been equidistributed. Digital filters are employed to process the residual as well as the density to ensure the regularity of the grid. Once $\varphi(\tau)$ is determined, another control law determines N based on the prescribed tolerance TOL , by adding appropriately many points distributed according to $\varphi(\tau)$. Here, the aim is to have the global error satisfying the tolerance requirement. It turns out that the procedure produces a near-optimal grid in a stable manner and also predicts how many grid points are needed. Numerical tests demonstrate the advantages of the new control system within the `bvpsuite` solver for a selection of problems and over a wide range of tolerances [49].

1.3.5 Pathfollowing for parameter dependent problems

To describe the strategy in general terms, we interpret the BVP as a parameter-dependent operator equation.

$$F(y; \lambda) = 0,$$

where $F : Y \times \mathbb{R} \rightarrow Z$, and Y, Z are Banach spaces (of possibly infinite dimension). Pathfollowing in this general setting has been discussed in detail in [59] and with singular BVP at [58]. While following a path in the solution-parameter space, we are often interested in computing solution branches Γ showing the so-called *turning points*. In a turning point the solution of $F(y; \lambda) = 0$ constitutes a local maximum (or minimum) of the parameter λ , and consequently is not locally unique as a function of λ . This means that increasing (or decreasing) its values and then trying to find the related solution cannot be successful. In such a case, it is useful to choose arclength to parameterize the curve. Following [35], we assume that we have found a starting solution-parameter pair $(y_0, \lambda_0) \in \Gamma$. In order to find the next approximation pair $(y_1, \lambda_1) \in \Gamma$, we make a step in the tangent direction in the point (y_0, λ_0) and obtain the predictor point (y_P, λ_P) . Finally, we project the predictor point into Γ in the direction which is perpendicular to the tangent in (y_P, λ_P) . This yields the correction point $(y_C, \lambda_C) =: (y_1, \lambda_1) \in \Gamma$.

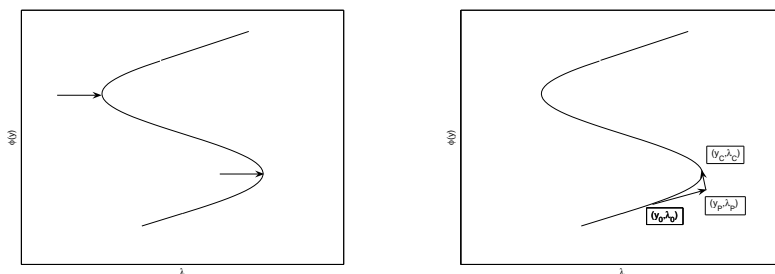


Figure 2: A solution branch with two turning points (left), one step of the pathfollowing procedure (right).

2 Computational Approaches to Singular Free Boundary Problems in Ordinary Differential Equations

2.1 Introduction

Many mathematical models in physics and mechanics lead to the following free boundary problem: find a real $M > 0$ and a positive solution of the equation

$$(|y'|^{m-2} y')' + \frac{N-1}{x} |y'|^{m-2} y' + f(y) = 0, \quad 0 < x < M, \quad (22)$$

which belongs to $C^2((0, M)) \cap C^1([0, M])$ and satisfies the boundary conditions

$$y'(0) = 0, \quad y(M) = y'(M) = 0, \quad M > 0. \quad (23)$$

In (22), N is the space dimension ($N \geq 2$), $m > 1$ and

$$f(y) = ay^q - by^p, \quad (24)$$

where $p < q$ and $a, b > 0$. When $m = 2$, equation (22) reduces to

$$y'' + \frac{N-1}{x} y' + f(y) = 0, \quad 0 < x < M, \quad (25)$$

where the differential operator on the left-hand side is the Laplacian in polar coordinates. In the general case, when $m \neq 2$, this operator becomes the so-called degenerate m -Laplacian. Results about existence and uniqueness of the solution of this problem can be found in [24].

In [46] and [42] the problem (22)–(23) has been studied in more detail. Special attention has been paid to the singularities (at $x = 0$ and $x = M$). Asymptotic expansions of the solution have been obtained about these points and based on these expansions, smoothing variable transformations have been proposed in [46]. In the latter paper a numerical method has been proposed, where the smoothing variable transformations are applied and the problem is discretized by means of a finite difference scheme.

The aim of this section is to obtain the numerical solution of problem (22)–(23) using the `bvpsuite` solver, based on collocation methods and designed for singular problems. The `bvpsuite` code has the ability to solve ODEs in implicit forms (see Subsection 1.3) and is therefore well suited for the considered numerical examples (see Subsection 2.3), furthermore it was successfully applied to the solution of a BVP for equation (22) on an unbounded domain [26].

With the purpose of applying the method mentioned above, we rewrite equations (22)–(23) in the new variable $z = x/M$, by dividing (22) by the factor $|y'(z)|^{m-2}$:

$$y''(z) + \frac{1}{m-1} \frac{N-1}{z} y'(z) + \frac{1}{m-1} \lambda \frac{f(y)}{|y'(z)|^{m-2}} = 0, \quad 0 < z < 1, \quad (26)$$

$$y'(0) = 0, \quad y(1) = y'(1) = 0, \quad (27)$$

where $\lambda = M^m$ is called eigenvalue² of the problem. In this case, our aim is to find a value λ , such that a positive solution of equation (26) exists, for which the conditions (27) are satisfied. By formulating the problem in the form (26)–(27) and applying the smoothing variable transformations to the resulting equations, described in [42], we obtain a new BVP, to which the `bvpsuite` code can be applied.

Finally, the described numerical scheme was used to solve a set of test cases, which were previously computed by the finite differences method, so that we can compare the performance of both computational algorithms. Since the order of convergence is an important criterion for a comparison, we used equidistant meshes with the initial stepsize $h = 0.01$ and estimated the convergence order by successive halving of the stepsizes.

2.2 Variable Substitution

Concerning singularities, four different situations may arise in the considered problem:

- **Case A.** If $m \leq 2$ and $p \geq m/2 - 1$: the solution is smooth at both endpoints;
- **Case B.** If $m \leq 2$ and $p < m/2 - 1$: the solution is regular at $z = 0$ and singular at $z = 1$;
- **Case C.** If $m > 2$ and $p \geq m/2 - 1$: the solution is singular at $z = 0$ and smooth at $z = 1$;
- **Case D.** If $m > 2$ and $p < m/2 - 1$, the solution is singular at both endpoints.

For each case, there is a family of variable substitutions which transforms the solution of the problem into a smooth function (see [42]). Since the Case D is the most general one, the corresponding family of variable substitutions contains the other ones. This family is described by the following formula:

$$t = \left(1 - (1 - z)^{\frac{k_2}{2}}\right)^{\frac{k_1}{2}}, \quad (28)$$

where $k_1 = \frac{m}{m-1}$ and $k_2 = \frac{m}{m-1-p}$. After introducing this variable substitution into equation (26), we obtain

$$\begin{aligned} a_1(t) |y'(t)|^{m-2} [b_1(t)y''(t) + c_1(t)y'(t)] + \lambda(ay(t)^q - by(t)^q) &= 0, \\ y'(0) &= 0, \\ y(1) = y'(1) &= 0, \end{aligned} \quad (29)$$

where

²Since the solution of the problem is unique, λ is not an eigenvalue in the usual sense.

$$\begin{aligned}
a_1(t) &= (m-1) \left(\frac{k_1 k_2}{4} \right)^{m-1} t^{\left(1-\frac{2}{k_1}\right)(m-1)} \left(1-t^{\frac{2}{k_1}}\right)^{\left(1-\frac{2}{k_2}\right)(m-1)}, \\
b_1(t) &= \frac{k_1 k_2}{4} t^{1-\frac{2}{k_1}} \left(1-t^{\frac{2}{k_1}}\right)^{1-\frac{2}{k_2}}, \\
c_1(t) &= \frac{1}{4} t^{-\frac{2}{k_1}} \left(1-t^{\frac{2}{k_1}}\right)^{-\frac{2}{k_2}} \left[4-2k_2 + \left(1-t^{\frac{2}{k_1}}\right)(-4+k_1 k_2)\right] + \\
&\quad + \frac{N-1}{(m-1) \left(1-\left(1-t^{\frac{2}{k_1}}\right)^{\frac{2}{k_2}}\right)}.
\end{aligned} \tag{30}$$

For sake of simplicity, in (29) the prime denotes differentiation with respect to the new variable t (while it denotes derivation with respect to z in equations (26)–(27)). Note that the variable substitution to be applied in Case B (resp. C) is a particular case of (28) with $k_1 = 2$ (resp., $k_2 = 2$).

2.3 Numerical Examples

2.3.1 Numerical Example 1

As a first example, we consider the case $p = -\frac{1}{2}$, $q = 1$, $a = 1$, $b = 1$, $m = \frac{3}{2}$, $N = 3$. In this case, the original equation has the form

$$y''(z) + \frac{4}{z} y'(z) + 2\lambda \left(y(z) - \frac{1}{\sqrt{y(z)}} \right) \sqrt{|y'(z)|} = 0, \tag{31}$$

with boundary conditions

$$y'(0) = y'(1) = y(1) = 0. \tag{32}$$

It is easy to check that the solution of this problem is nonsmooth at $z = 1$. We were unsuccessful in solving (31) using the `bvpsuite` code, the algorithm did not converge (even if the iterative process was started with the transformed solution of the smooth problem).

We have then applied the variable substitution $t = 1 - (1-z)^{\frac{3}{4}}$ to the problem (31), which yields

$$\begin{aligned}
\frac{3\sqrt{3}}{16\sqrt{1-t}} y''(t) + \left(\frac{\sqrt{3}}{16(1-t)^{\frac{3}{2}}} + \frac{\sqrt{3}}{(1-t)^{\frac{1}{6}} \left(1 - (1-t)^{\frac{4}{3}}\right)} \right) y'(t) + \\
+ \lambda \sqrt{|y'(t)|} \left(y(z) - \frac{1}{\sqrt{y(t)}} \right) = 0, \\
y'(0) = y'(1) = y(1) = 0.
\end{aligned} \tag{33}$$

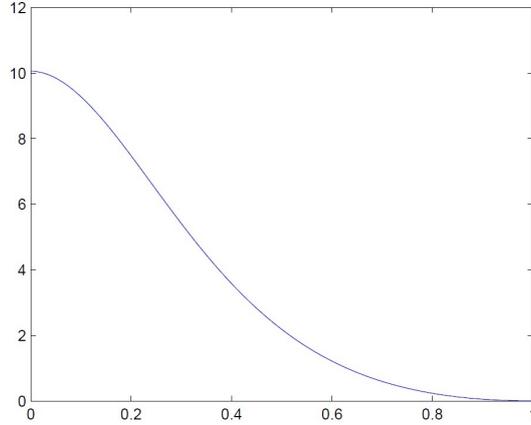


Figure 3: Graph of the numerical solution of the modified problem for Example 1.

It turns out that the solution of problem (33) is smooth in the whole interval $[0, 1]$.

The collocation method with one Gaussian point was successfully applied to the solution of this problem. The numerical results are displayed in Table 1. We provide the errors of the approximations of the solutions and the constants λ . Since we do not know the exact solution, the errors are computed with respect to the numerical solution, obtained on 12801 subintervals. In both cases (approximated solutions and constants λ) the numerical results suggest second order convergence. This is the same convergence order that was obtained when solving the same problem using the finite differences method (see [42]). We have tried to apply higher order collocation methods to this problem, but the algorithm did not converge with any initial approximation.

The graph of the numerical solution of the modified problem can be found in Figure 3.

intervals	error	rate	error λ	rate λ
101	1.4159e-3	-	7.7077e-4	-
201	3.7705e-4	1.9089	2.0018e-4	1.9450
401	9.8751e-5	1.9329	5.1658e-5	1.9542
801	2.5368e-5	1.9608	1.3163e-5	1.9725
1601	6.2294e-6	2.0258	3.2199e-6	2.0315

Table 1: Numerical results for Example 1 in the modified version.

2.3.2 Numerical Example 2

We will now consider the case $p = \frac{1}{2}$, $q = 1$, $a = 1$, $b = 1$, $m = 3$, $N = 3$, when the original equation has the form

$$\begin{aligned} y''(z) + \frac{1}{z} y'(z) + \frac{\lambda}{2} \frac{y(z) - \sqrt{y(z)}}{|y'(z)|} &= 0, \\ y'(0) &= 0, \\ y'(1) = y(1) &= 0. \end{aligned} \tag{34}$$

The analytical solution of (34) is known,

$$y(z) = \left(2 - 2z^{\frac{3}{2}}\right)^2, \quad \lambda = 216, \quad y \in C^2(0, 1]. \tag{35}$$

This solution is not smooth at $z = 0$.

The collocation method with one Gaussian point was successfully applied to solve this problem. The numerical results are displayed in Table 2.

intervals	error	rate	error λ	rate λ
101	2.4592e-03	-	2.2481e-02	-
201	9.0740e-04	1.4594	5.8931e-03	1.9316
401	3.2732e-04	1.4710	1.58931e-03	1.9253
801	1.1738e-04	1.4795	4.0867e-04	1.9247
1601	4.1922e-05	1.4855	1.0751e-04	1.9265

Table 2: Numerical results for Example 2 in the original version.

In order to deal with the singularity at $z = 0$ and improve the performance of the numerical method, we introduce the variable substitution $t = z^{\frac{3}{4}}$, which reduces equation (34) to the form

$$\begin{aligned} \frac{27}{32t} y''(t) + \frac{27}{32t^2} y'(t) + \lambda \frac{y(t) - \sqrt{y(t)}}{|y'(t)|} &= 0, \\ y'(0) &= 0, \\ y'(1) = y(1) &= 0. \end{aligned} \tag{36}$$

It can easily be checked that the exact solution of (36) is

$$y(t) = (2 - 2t^2)^2, \quad \lambda = 216, \quad y \in C^\infty[0, 1]. \tag{37}$$

In the case of Example 2, we have obtained numerical results both for the original and the modified problem. As it could be expected, when applying the collocation method to the modified problem, the accuracy of the results is significantly improved (for further details, see Subsection 2.3.5). We have applied the following variants of the collocation method: 1 Gaussian point ($\mu = 2$), 2 Gaussian points ($\mu = 3$), 3 Gaussian points ($\mu = 4$), 2 equidistant points ($\mu = 3$), and 3 equidistant points ($\mu = 4$) (here μ denotes the degree of the corresponding collocation polynomial). The numerical results are displayed in the Tables 3 to 7.

The rates in the Tables 5 and 7 are of course without meaning. Even with just fifty intervals the numerical solution is strongly influenced from rounding errors (which increasingly occur with higher order schemes). A meaningful rate of convergence cannot be reasonably expected. Again, we displayed the maximal errors of the approximations of the solutions and the constants λ .

intervals	error	rate	error λ	rate λ
101	7.64118e-5	-	6.8103e-3	-
201	1.9027e-5	2.0058	2.6333e-3	1.3708
401	4.9672e-6	1.9376	8.9147e-4	1.5626
801	1.4116e-6	1.8151	2.8124e-4	1.6644
1601	4.0686e-7	1.7948	8.4917e-5	1.7277

Table 3: Numerical results for Example 2 in the modified version calculated with one Gaussian point.

intervals	error	rate	error λ	rate λ
101	7.9716e-9	-	1.4811e-6	-
201	8.7822e-10	3.1822	1.7467e-7	3.0839
401	1.0315e-10	3.0898	2.1428e-8	3.0271
801	1.2486e-11	3.0464	2.6561e-9	3.0121
1601	1.5401e-12	3.0192	3.3262e-10	2.9974

Table 4: Numerical results for Example 2 in the modified version calculated with two Gaussian points.

intervals	error	rate	error λ	rate λ
101	3.9817e-12	-	5.7554e-11	-
201	9.4458e-13	2.0756	4.3201e-11	0.4139
401	1.9007e-13	2.3131	1.2136e-11	1.8318
801	6.7457e-13	-1.8274	8.5151e-11	-2.8107
1601	1.0614e-13	2.6680	1.5859e-11	2.4247

Table 5: Numerical results for Example 2 in the modified version calculated with three Gaussian points.

intervals	error	rate	error λ	rate λ
101	6.6660e-5	-	3.5895e-3	-
201	1.6666e-5	1.9999	8.9860e-4	1.9980
401	4.1666e-6	2.0000	2.2482e-4	1.9989
801	1.0417e-6	2.0000	5.6227e-5	1.9994
1601	2.6041e-7	2.0001	1.4058e-5	1.9998

Table 6: Numerical results for Example 2 in the modified version calculated with two equidistant points.

intervals	error	rate	error λ	rate λ
101	1.6653e-12	-	3.1406e-11	-
201	4.8939e-13	1.7668	1.8417e-11	0.7700
401	2.3928e-12	-2.2896	2.5145e-10	-3.7711
801	3.9613e-13	2.5946	4.7919e-11	2.3916
1601	5.7732e-14	2.7785	8.7255e-12	2.4573

Table 7: Numerical results for Example 2 in the modified version calculated with three equidistant points.

In the following figures, the errors corresponding to each variant are denoted by 'errorg1', 'errorg2', 'errorg3', 'errora1' and 'errora3', respectively. For Example 2, concerning the numerical approximations of the solutions and the constants λ , the performance of these algorithms is illustrated in Figures 4 and 5.

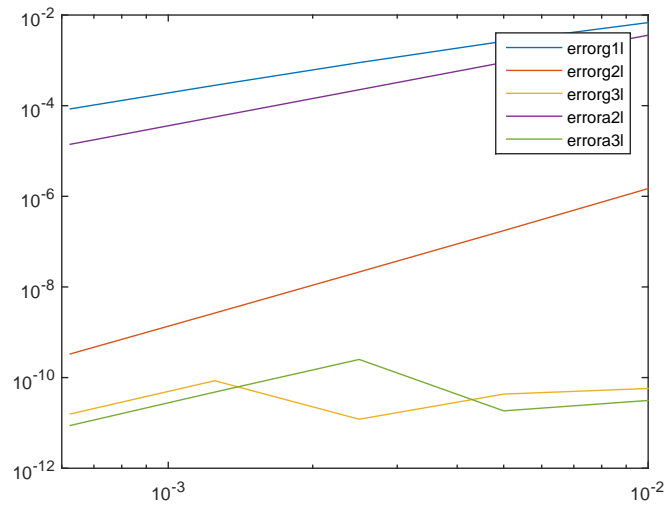


Figure 4: Graphs of the estimated errors of λ of the modified problem for Example 2.

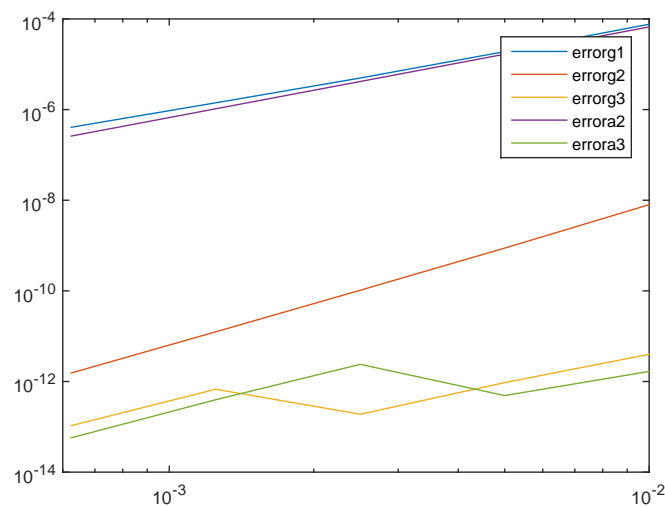


Figure 5: Graphs of the estimated errors of the numerical solution of the modified problem for Example 2.

The graphs of the numerical solutions of the original and modified problem are displayed in Figure 6 (note that we are representing in the same axis two different independent variables: z , in the case of the original problem, and t , in the case of the modified one).

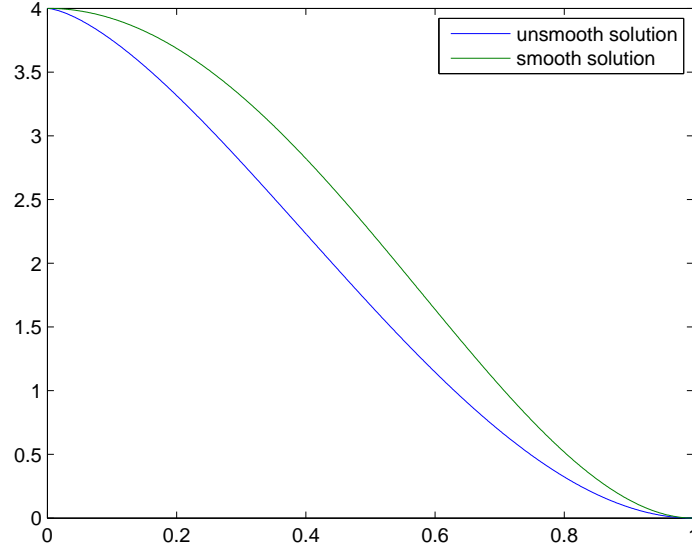


Figure 6: Graphs of the numerical solution of the original (unsmooth) and modified (smooth) problem for Example 2.

2.3.3 Numerical Example 3

As the third numerical example, we have considered the case $p = 1 - \alpha = -\frac{1}{2}$, $q = 1$, $a = 1$, $b = \frac{1}{\alpha} = \frac{2}{3}$, $m = 2$, $N = 1$. In this case, the original problem can be written as

$$y''(z) + \lambda \left(y(z) - \frac{2}{3\sqrt{y(z)}} \right) = 0, \quad y'(0) = y'(1) = y(1) = 0. \quad (38)$$

As in the previous case the exact solution is also known:

$$y(z) = \left(\frac{8}{3} \right)^{\frac{2}{3}} \left(\cos \left(\frac{\pi}{2} z \right) \right)^{\frac{4}{3}}, \quad \lambda = \left(\frac{2\pi}{3} \right)^2, \quad y \in C^2(0, 1]. \quad (39)$$

This solution is not smooth at $z = 0$. When the collocation method is applied to the problem (38), numerical results can be obtained, but the convergence rate is poor (see the discussion in Subsection 2.3.5).

intervals	error	rate	error λ	rate λ
101	8.3303e-3	-	3.7032e-2	-
201	4.3873e-3	0.9250	1.9546e-2	0.9219
401	2.3349e-3	0.9100	1.0446e-2	0.9039
801	1.2575e-3	0.8928	5.6538e-3	0.8857
1601	6.8627e-4	0.8738	3.0999e-3	0.8670

Table 8: Numerical results for Example 3 in the original version calculated with one Gaussian point.

In this case, the adequate variable substitution, to deal with the singularity at $z = 0$, is $t = 1 - (1 - z)^{\frac{2}{3}}$. After applying this variable substitution the problem (38) is reduced to

$$\begin{aligned} \frac{4}{9(1-t)}y''(t) + \frac{2}{9(t-1)^2}y'(t) + \lambda \left(y(t) - \frac{2}{3\sqrt{y(t)}} \right) &= 0, \\ y'(0) &= 0, \\ y'(1) = y(1) &= 0, \end{aligned} \tag{40}$$

which has the exact solution

$$y(t) = \left(\frac{8}{3} \right)^{\frac{2}{3}} \left(\cos \left(\frac{\pi}{2} \left(1 - (1-t)^{\frac{3}{2}} \right) \right) \right)^{\frac{4}{3}}, \tag{41}$$

with

$$\lambda = \left(\frac{2\pi}{3} \right)^2, \quad y \in C^\infty[0, 1].$$

As in the previous example, the application of the variable substitution results in a significant improvement of the accuracy of the numerical results.

The numerical results are displayed in the Tables 9 to 13. In Table 13 the so-called small superconvergence order $m + 1$ can be observed, since superconvergence cannot be expected to hold for singular problems, in general. More details are given in Subsection 2.3.5.

intervals	error	rate	error λ	rate λ
101	8.8583e-5	-	2.3858e-4	-
201	2.2148e-5	1.9998	5.9653e-5	1.9998
401	5.5372e-6	2.0000	1.4914e-5	1.9999
801	1.3843e-6	2.0000	3.7285e-6	2.0000
1601	3.4608e-7	2.0000	9.3214e-7	2.0000

Table 9: Numerical results for Example 3 in the modified version calculated with one Gaussian point.

intervals	error	rate	error λ	rate λ
101	2.8173e-9	-	9.8280e-9	-
201	1.9893e-10	3.8239	7.2363e-10	3.7636
401	1.3860e-11	3.8433	5.2265e-11	3.7913
801	9.5612e-13	3.8575	3.7188e-12	3.8129
1601	6.4615e-14	3.8873	2.6823e-13	3.7933

Table 10: Numerical results for Example 3 in the modified version calculated with two Gaussian points.

intervals	error	rate	error λ	rate λ
101	1.5255e-11	-	6.7401e-11	-
201	7.7360e-13	4.3015	3.4754e-12	4.2775
401	3.9413e-14	4.2949	1.7586e-13	4.3047
801	2.2204e-15	4.1497	5.3291e-15	5.0444
1601	3.2196e-15	-0.5361	7.1054e-15	-0.4150

Table 11: Numerical results for Example 3 in the modified version calculated with three Gaussian points.

intervals	error	rate	error λ	rate λ
101	4.2174e-5	-	6.1834e-5	-
201	1.0544e-5	2.0000	1.5460e-5	1.9999
401	2.6359e-6	2.0000	3.8649e-6	2.0000
801	6.5898e-7	2.0000	9.6624e-7	2.0000
1601	1.6475e-7	2.0000	2.4156e-7	2.0000

Table 12: Numerical results for Example 3 in the modified version calculated with two equidistant points.

intervals	error	rate	error λ	rate λ
101	2.2610e-9	-	4.0703e-9	-
201	1.5031e-10	3.9110	2.9400e-10	3.7912
401	9.9575e-12	3.9160	2.0850e-11	3.8177
801	6.5759e-13	3.9205	1.4522e-12	3.8438
1601	4.2855e-14	3.9397	1.0036e-13	3.8549

Table 13: Numerical results for Example 3 in the modified version calculated with three equidistant points.

The performance of the 5 variants of the collocation method (see description in Subsection 2.3.2) is compared in Figures 7 and 8. The graphs of the solutions of the original and modified problem are displayed in Figure 9.

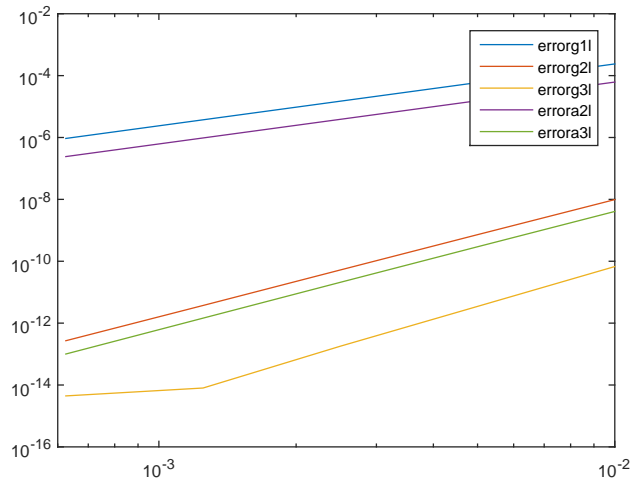


Figure 7: Graphs of the estimated errors of λ of the modified problem for Example 3.

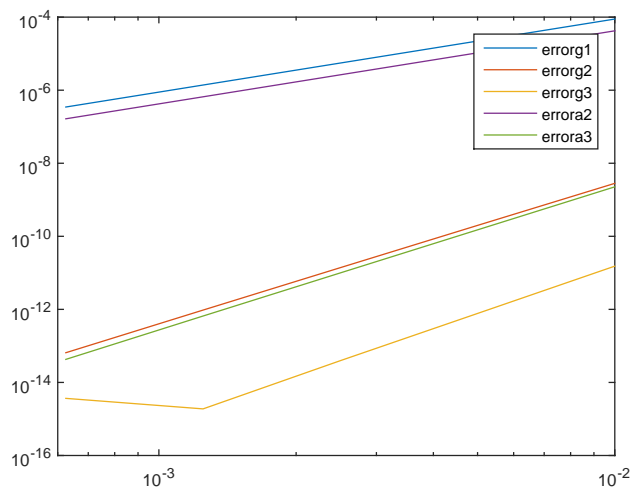


Figure 8: Graphs of the estimated errors of the numerical solution of the modified problem for Example 3.

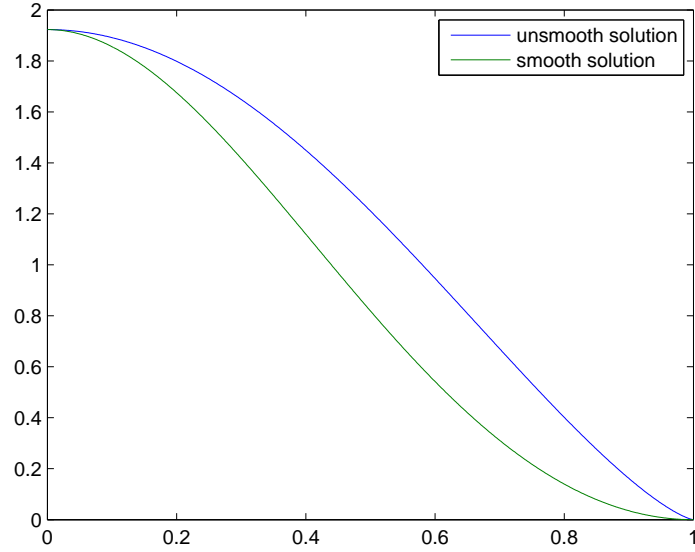


Figure 9: Graphs of the numerical solution of the original (unsmooth) and modified (smooth) problem for Example 3.

2.3.4 Numerical Example 4

The final example is the case $p = 0$, $q = 1$, $a = 1$, $b = 1$, $m = 3$, $N = 3$, for which the exact solution is not known in closed form. The problem may be written as

$$\begin{aligned}
 y''(z) + \frac{1}{z} y'(z) + \frac{\lambda}{2} \frac{y(z) - 1}{|y'(z)|} &= 0, \\
 y'(0) &= 0, \\
 y'(1) = y(1) &= 0.
 \end{aligned} \tag{42}$$

In this case the solution is nonsmooth in both endpoints. As in Example 1, the collocation algorithm failed to produce a numerical solution when applied to problem (42). Since we are in Case D (the solution is unsmooth in both endpoints in this case), we must apply the variable substitution $t = \left(1 - (1 - z)^{\frac{3}{4}}\right)^{\frac{3}{4}}$. After this transformation is applied,

we obtain

$$\begin{aligned}
& \frac{729}{2048t\left(1-t^{\frac{4}{3}}\right)}y''(z)+ \\
& + \left(\frac{81}{512t^{\frac{2}{3}}\left(1-t^{\frac{4}{3}}\right)^2} - \frac{243}{2048t^2\left(1-t^{\frac{4}{3}}\right)} + \frac{81}{128t^{\frac{2}{3}}\left(1-t^{\frac{4}{3}}\right)^{\frac{2}{3}}\left(1-\left(1-t^{\frac{4}{3}}\right)^{\frac{4}{3}}\right)} \right) y'(z)+ \\
& + \lambda \frac{y(z)-1}{|y'(z)|} = 0, \\
& y'(0) = y'(1) = y(1) = 0.
\end{aligned} \tag{43}$$

The solution of problem (43) is smooth on the whole interval $[0, 1]$. Once again, the application of the variable substitution enables us to solve the problem by the collocation method.

intervals	error	rate	error λ	rate λ
101	2.9690e-4	-	1.0392e-2	-
201	7.4201e-5	2.0005	2.6481e-3	1.9724
401	1.8546e-5	2.0003	6.7276e-4	1.9768
801	4.6362e-6	2.0001	1.7044e-4	1.9808
1601	1.1590e-6	2.0001	4.3074e-5	1.9844

Table 14: Numerical results for Example 4 in the modified version calculated with one Gaussian point.

intervals	error	rate	error λ	rate λ
101	5.4169e-8	-	4.094e-6	-
201	1.4366e-8	1.9148	1.1438e-6	1.8398
401	2.8523e-9	2.3325	2.3390e-7	2.2898
801	5.0821e-10	2.4886	4.2424e-8	2.4629
1601	8.5791e-11	2.5665	7.2407e-9	2.5507

Table 15: Numerical results for Example 4 in the modified version calculated with two Gaussian points.

intervals	error	rate	error λ	rate λ
101	1.1207e-8	-	8.8462e-7	-
201	1.7684e-9	2.6639	1.4439e-7	2.6151
401	2.7833e-10	2.6676	2.3178e-8	2.6391
801	4.3667e-11	2.6722	3.6801e-9	2.6549
1601	6.7282e-12	2.6983	5.7172e-10	2.6864

Table 16: Numerical results for Example 4 in the modified version calculated with three Gaussian points.

intervals	error	rate	error λ	rate λ
101	2.2185e-4	-	5.2113e-4	-
201	5.6331e-5	1.9776	1.3283e-4	1.9721
401	1.4155e-5	1.9926	3.3596e-5	1.9832
801	3.5504e-6	1.9953	8.4587e-6	1.9898
1601	8.8786e-7	1.9996	2.1239e-6	1.9937

Table 17: Numerical results for Example 4 in the modified version calculated with two equidistant points.

intervals	error	rate	error λ	rate λ
101	5.5612e-8	-	8.924e-8	-
201	5.8860e-9	3.2400	1.0583e-8	3.076
401	6.0731e-10	3.2768	1.2189e-9	3.1180
801	6.1770e-11	3.2975	1.3532e-10	3.1712
1601	6.5854e-12	3.2296	1.5497e-11	3.1263

Table 18: Numerical results for Example 4 in the modified version calculated with three equidistant points.

We again apply the 5 variants of the collocation method considered in previous examples (see Tables 14 to 18). Figures 10 and 11 illustrate the performance of these methods in the case of Example 4. The graph of the numerical solution of the modified problem is shown in Figure 12.

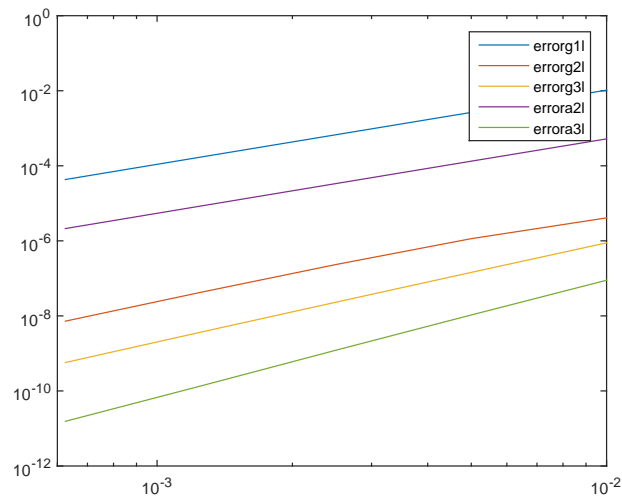


Figure 10: Graphs of the estimated errors of λ of the modified problem for Example 4.

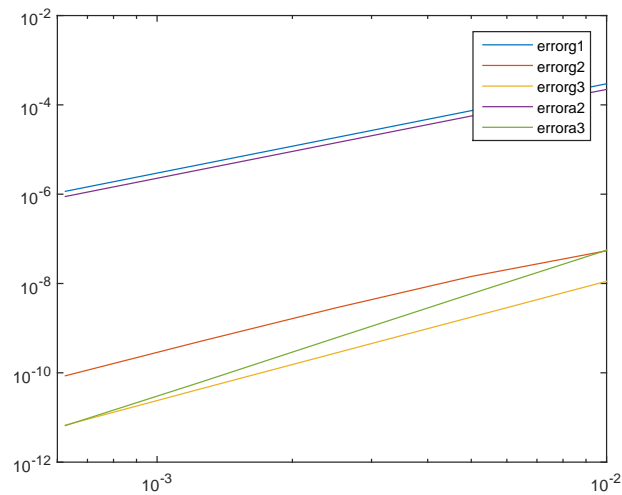


Figure 11: Graphs of the estimated errors of the numerical solution of the modified problem for Example 4.

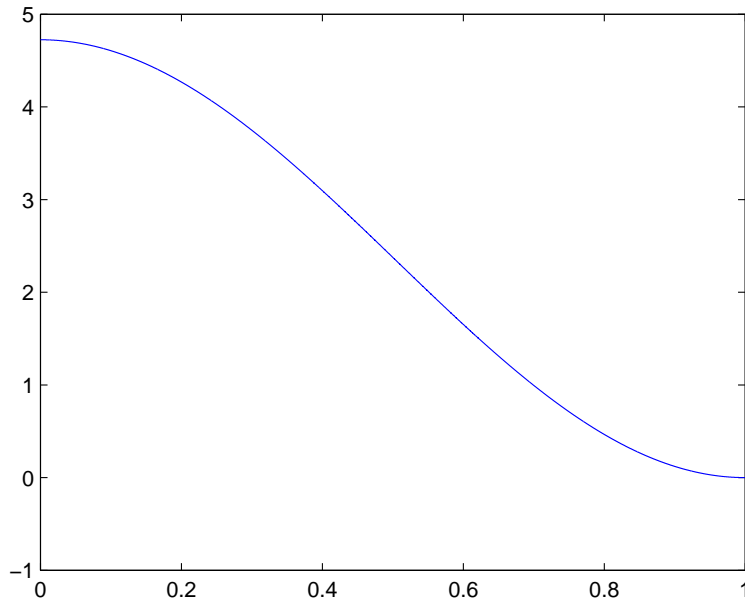


Figure 12: Graph of the numerical solution of the modified problem for Example 4.

2.3.5 Summary of Numerical Results

We have considered four numerical examples of singular problems and solved them by using collocation methods. In particular, we have observed that the performance of the numerical method is always better after applying the variable substitution smoothing the solution. To complete the picture, in Table 19 we display a comparison of the numerical results for all the 4 examples, obtained by each of the 5 methods. To compare the accuracy of the methods, we use the estimated convergence rate. For each method and example, we have used meshes with $N = 101, \dots, N = 1601$ points. This allows us to compute, for each case, 4 different estimates of the convergence rate. In Table 19 we give an approximate extrapolated value of these estimates. In certain cases, we have observed a large variation of the estimates, which probably means that the computed values are strongly affected by rounding-off errors and the extrapolation of these values may not make sense. These cases were just marked by '??'. The meaning of the abbreviations in Table 19 is: o.p. - original problem; m.p. - modified problem; g - Gaussian points; e - equidistant points; μ is the degree of the collocation polynomial.

	Example 1	Example 2	Example 3	Example 4
o.p., g., $\mu = 2$	no conv.	2	1	no conv.
m.p.,g., $\mu = 2$	2	2	2	2
m.p.,g., $\mu = 3$	no conv.	3.0	3.8	2.5
m.p.,g., $\mu = 4$	no conv.	??	5.0	2.7
m.p.,e., $\mu = 3$	no conv.	2	2	2
m.p.,e., $\mu = 4$	no conv.	??	3.8	??

Table 19: Estimates of the convergence order for each example by different methods.

2.4 Conclusions

We have implemented a new numerical method for the computation of approximate solutions to singular free boundary problems in ODEs, using the open domain MATLAB code `bvpsuite`. Our numerical approach is based on smoothing variable transformations which transplant the original problem with endpoint singularities into a new problem, whose solution is smooth in the whole interval.

As illustrated by the numerical examples, when solving the modified problem the performance of the collocation method is always better than if it is applied to the original one. Even in the cases in which the numerical method fails to approximate the original problem, accurate results are obtained after applying the variable transformation.

As shown by the numerical results, the approximations obtained using the collocation method (combined with the variable substitution) have convergence order not less than two, both for the solutions and the constant λ . However, it is not always possible to recover the optimal convergence order of the collocation method, as it was previously observed in the case of boundary value problems with the p -Laplacian [26].

When the collocation method is used with 1 Gaussian point, $\mu = 2$, or 2 equidistant points, $\mu = 3$, the numerical results suggest second order convergence, the same which is obtained when the finite differences method is applied (see [42]). By increasing the degree of the collocation polynomial μ , the accuracy of the approximations is significantly improved in most of the numerical examples. However, it is not always clear from the numerical results what is the convergence order of the method.

3 Solving the generalized Korteweg-de Vries equation with `bvpsuite`

3.1 Introduction

In this section, we analyse the Generalized Korteweg-de Vries (GKdV) equation of the following form

$$u_t + u_{xxx} + u^p u_x = 0, \quad x \in \mathbb{R}, \quad t \geq 0, \quad (44)$$

where $u = u(x, t)$, $p \in \mathbb{N}$, $p \geq 1$ and with the initial condition

$$u(x, 0) = u_0(x), \quad x \in \mathbb{R}. \quad (45)$$

This equation arises in modelling the propagation of small-amplitude waves in a variety of nonlinear dispersive media, where u represents the wave amplitude, see [51, 14, 13]. Moreover, the equation is shown to describe the behaviour of longitudinal waves propagating in a one-dimensional lattice of equal masses coupled by nonlinear springs; the Fermi, Pasta, Ulam (FPU)-lattice, see [61] and references therein. The special case $p = 2$ gives the classical Korteweg-de Vries equation (KdV) which was posed by Korteweg and de Vries [39] to describe water waves on shallow water surfaces. The case $p = 3$, which is known as the Modified Korteweg-de Vries equation, can be transformed into the original Korteweg-de Vries equation by the Miura transformation, [1].

Together with the nonlinear Schrödinger equation, this equation can be considered as a universal model for Hamiltonian systems in infinite dimensions. Since equation (44) is Hamiltonian, the energy is conserved, where the energy is given by

$$\begin{aligned} E(u(t)) &= \frac{1}{2} \int_{\mathbb{R}} \left[u_x(x, t)^2 - \frac{1}{p+1} u(x, t)^{p+1} \right] dx \\ &= \frac{1}{2} \int_{\mathbb{R}} \left[u_x(x, 0)^2 - \frac{1}{p+1} u(x, 0)^{p+1} \right] dx. \end{aligned} \quad (46)$$

Moreover, the mass, given by

$$M(u(t)) = \int_{\mathbb{R}} u(x, t)^2 dx, \quad (47)$$

is also conserved, so

$$M(u(t)) = \int_{\mathbb{R}} u(x, 0)^2 dx. \quad (48)$$

In this section, we study solutions of equation (44) that become infinite in finite time, hence they blow up. The cases $p = 2$ and $p = 3$ are integrable and have already been studied extensively, see for example [41] and [44]. As a consequence of the Gagliardo-Nirenberg inequality, all solutions in $H^1(\mathbb{R})$ for $p < 5$ are global and bounded in time.

The choice $p = 5$ is the smallest power such that the prevailing conservation laws do not imply a bound in $H^1(\mathbb{R})$, uniform in time, for all H^1 -solutions and thus no global existence can be guaranteed. From this, blow-up in finite time is conjectured for $p \geq 5$, where $p = 5$ is the so-called critical power. Here we study blow-up solutions of equation (44) for $p \geq 5$. More specifically, we assume that the solutions blow up at some blow-up time $T < \infty$ where

$$\max_{x \in \mathbb{R}} |u(x, t)| \rightarrow \infty, \quad \text{as } t \rightarrow T, \quad (49)$$

with $|u(x, t)| < \infty$ for all $t < T, x \in \mathbb{R}$.

The blow-up rates observed in [15] strongly suggest a self-similar blow-up solution of the form

$$u(x, t) = \frac{1}{(T - t)^{2/(3(p-1))}} w \left(\frac{x}{(T - t)^{1/3}} \right). \quad (50)$$

Here, T is the blow-up time and the function $w = w(\xi)$, $\xi = \frac{x}{(T-t)^{1/3}}$, the similarity profile, satisfies the following nonlinear ordinary differential equation (ODE) subject to boundary conditions specified in (52):

$$\frac{2}{3(p-1)} w + \frac{\xi}{3} w_\xi + (w_{\xi\xi} + w^p)_\xi = 0, \quad \xi \in \mathbb{R}, \quad (51)$$

$$\frac{2}{3(p-1)} w(\xi) + \frac{\xi}{3} w_\xi(\xi) \xrightarrow{\xi \rightarrow \pm\infty} 0, \quad w_{\xi\xi}(\xi) \xrightarrow{\xi \rightarrow \infty} 0. \quad (52)$$

The aim is to find the function w satisfying the above boundary value problem (BVP) and defined for all $\xi \in \mathbb{R}$ by using the code `bvbsuite`, which has proven itself frequently for BVPs like (51)–(52). Since we want to solve the problem using mesh adaptation and need many plots with different parameters, `bvpsuite` seems to be the perfect tool with its mesh adaptation described in Subsection 1.3.4 and its easy to use graphical overview of all solution components on the grid.

3.2 Problem setting ($p \geq 6$)

Let us consider the BVP (51)–(52). We solve the problem using our open domain MATLAB code `bvpsuite` by reducing ξ to a finite interval $[-L, L]$ with a sufficiently large L ,

$$\frac{2}{3(p-1)} w + \frac{\xi}{3} w_\xi + (w_{\xi\xi} + w^p)_\xi = 0, \quad \xi \in (-L, L), \quad (53)$$

$$\frac{2}{3(p-1)} w(-L) - \frac{L}{3} w_\xi(-L) = 0, \quad \frac{2}{3(p-1)} w(L) + \frac{L}{3} w_\xi(L) = 0, \quad (54)$$

$$w_{\xi\xi}(L) = 0. \quad (55)$$

In the following table, we list the technical details for the run with the GUI; $p = 6$:

Field	Input value
Mesh	<code>linspace(-L, L, 10 * L)</code>
Equations	$z1d3 + 2/15 \cdot z1 + t/3 \cdot z1' + 6 \cdot z1^5 \cdot z1' = 0;$
Boundary / Additional conditions	$z1''(b) = 0; 2/15 \cdot z1(a) - L/3 \cdot z1'(a) = 0;$ $2/15 \cdot z1(b) + L/3 \cdot z1'(b) = 0;$
Initial Mesh	<code>linspace(-L, L, 10 * L)</code>
Initial values	<code>exp(-(linspace(-L, L, 10 * L).^2/10))</code>

Table 20: Settings for the MATLAB code `bvpsuite` GUI to reproduce the results for $p = 6$ and $L = 10$.

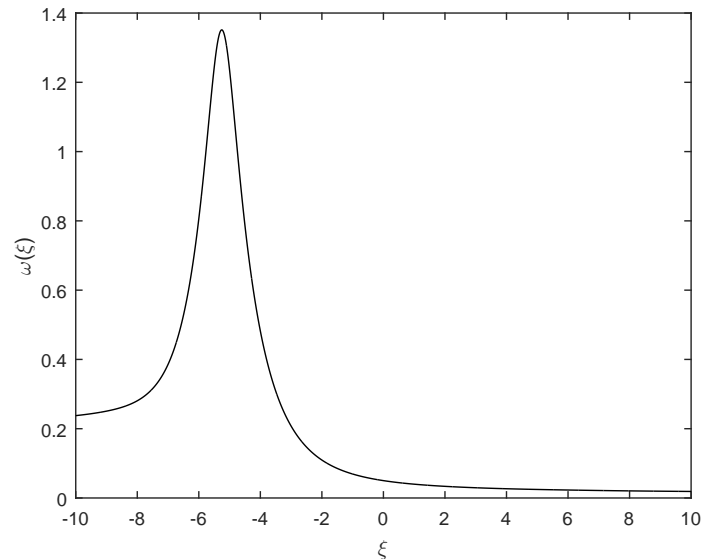
In the Tables 21 to 25, we show the estimated convergence order of the collocation scheme with one Gaussian point. Expected superconvergence order (maximal error taken over the mesh points only) $O(h^2)$ can be observed. The maximal error is estimated using the $h-h/2$ strategy. The related figures show the numerical solutions.

To see the influence of L , we increase L from $L = 10$ to $L = 50$ and check how the values $w(-6)$, $w(0)$ and $\|w\|_\infty$ change with L .

3.2.1 Convergence orders and plots of numerical solutions for $p = 6$

$50 \cdot h$	err_{abs}	ord
2^{-0}	$4.7900e - 02$	—
2^{-1}	$6.3000e - 03$	2.92
2^{-2}	$1.5000e - 03$	2.08
2^{-3}	$3.7090e - 04$	2.02
2^{-4}	$9.2430e - 05$	2.00

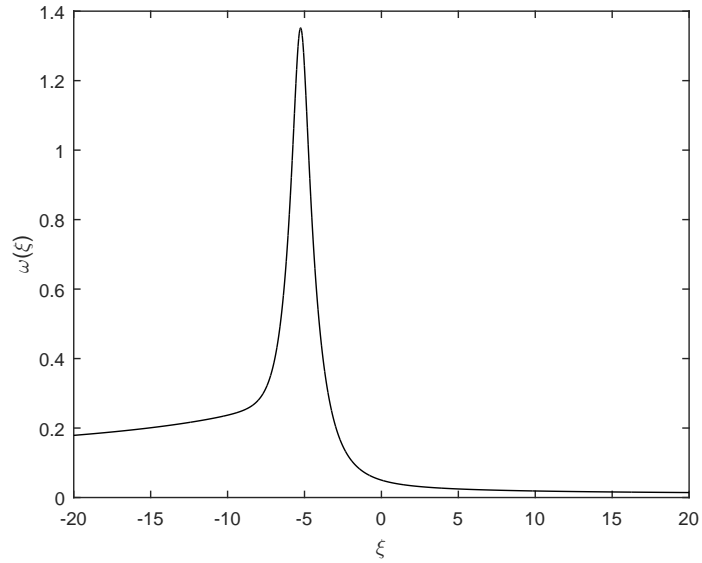
Table 21: $L = 10$



$$L = 10 : w(-6) = 0.8059, \quad w(0) = 0.0501, \quad \|w\|_\infty = w(-5.25) = 1.3515.$$

$50 \cdot h$	err_{abs}	ord
2^{-0}	$4.8300e - 02$	–
2^{-1}	$6.4000e - 03$	2.93
2^{-2}	$1.5000e - 03$	2.08
2^{-3}	$3.7155e - 04$	2.02
2^{-4}	$9.2590e - 05$	2.01

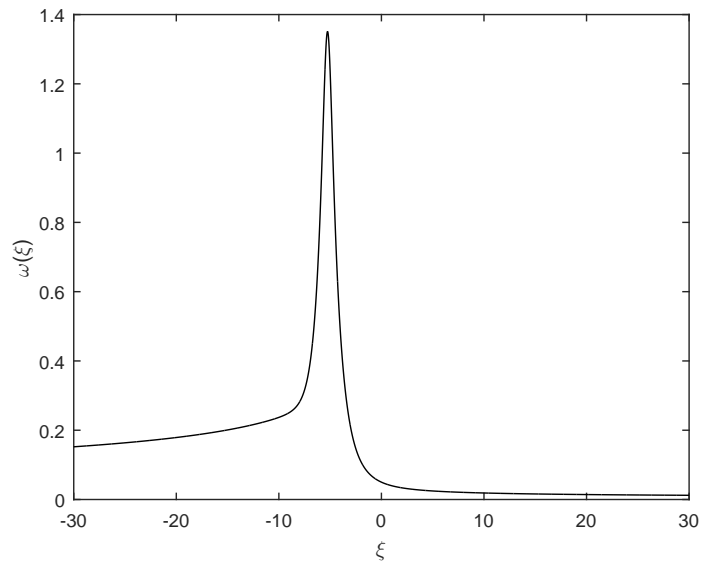
Table 22: $L = 20$



$$L = 20 : w(-6) = 0.8054, \quad w(0) = 0.0501, \quad \|w\|_{\infty} = w(-5.25) = 1.3515.$$

$50 \cdot h$	err_{abs}	ord
2^{-0}	$4.8200e - 02$	–
2^{-1}	$6.4000e - 03$	2.92
2^{-2}	$1.5000e - 03$	2.08
2^{-3}	$3.7143e - 04$	2.02
2^{-4}	$9.2560e - 05$	2.00

Table 23: $L = 30$



$$L = 30 : w(-6) = 0.8055, \quad w(0) = 0.0501, \quad \|w\|_{\infty} = w(-5.25) = 1.3515.$$

$$L = 40 : w(-6) = 0.8055, \quad w(0) = 0.0501, \quad \|w\|_{\infty} = w(-5.25) = 1.3515.$$

Note, that the solution w is quite unsmooth and it changes fast in the central region of the interval of integration. Since according to the above results, enlarging L beyond $L = 20$ has almost no influence, we fix $L = 20$ for the solution plots in the next section. In

$50 \cdot h$	err_{abs}	ord
2^{-0}	$4.8200e - 02$	—
2^{-1}	$6.4000e - 03$	2.92
2^{-2}	$1.5000e - 03$	2.08
2^{-3}	$3.7146e - 04$	2.02
2^{-4}	$9.2590e - 05$	2.00

Table 24: $L = 40$

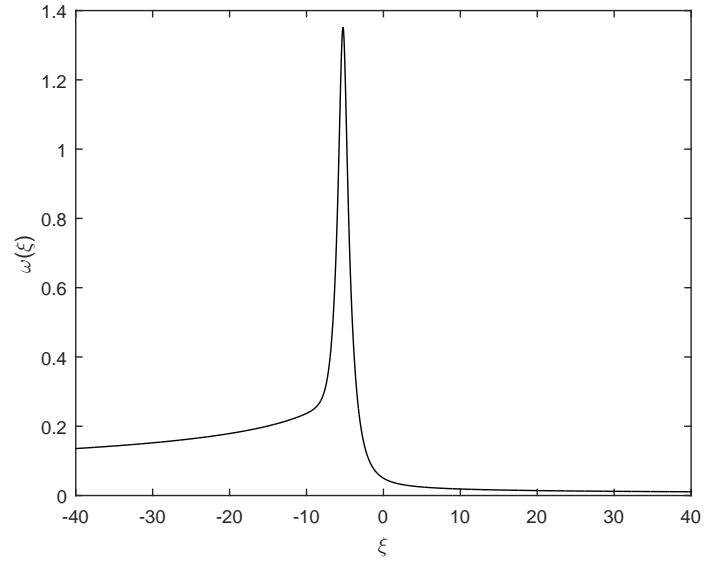
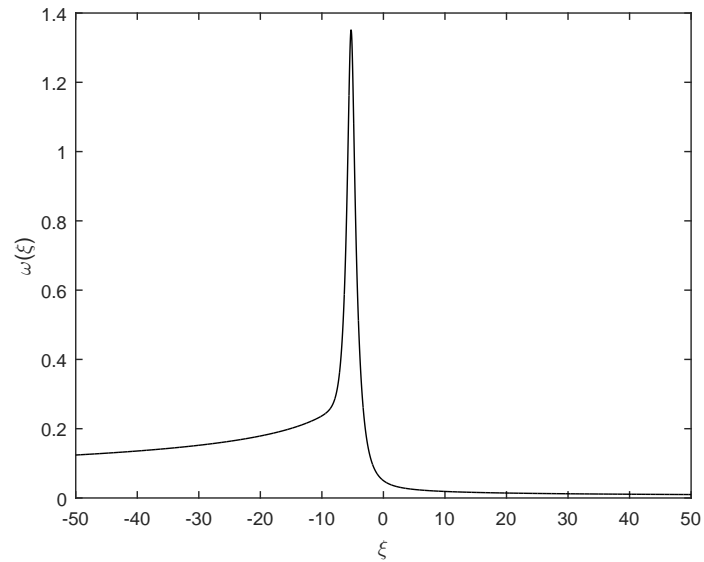


Table 26, we report on the empirical convergence orders for collocation at two and three equidistant collocation points and two Gaussian points. Classical convergence orders can be observed.

$50 \cdot h$	err_{abs}	ord
2^{-0}	$4.8200e - 02$	—
2^{-1}	$6.3000e - 03$	2.92
2^{-2}	$1.5000e - 03$	2.08
2^{-3}	$3.7120e - 04$	2.02
2^{-4}	$9.2503e - 05$	2.00

Table 25: $L = 50$



$L = 50 : w(-6) = 0.8055, \quad w(0) = 0.0501, \quad \|w\|_{\infty} = w(-5.25) = 1.3515.$

$50 \cdot h$	err _{a2}	ord		err _{a3}	ord		err _{g2}	ord
2^{-0}	$1.8600e-02$	—		$1.1300e-02$	—		$1.6601e-05$	—
2^{-1}	$2.6000e-03$	2.86		$1.9915e-05$	9.15		$3.2406e-05$	-0.97
2^{-2}	$6.5774e-04$	2.00		$1.2560e-06$	3.99		$2.0160e-06$	4.01
2^{-3}	$1.6427e-04$	2.00		$7.8684e-08$	4.00		$1.2554e-07$	4.01
2^{-4}	$4.1061e-05$	2.00		$4.9202e-09$	4.00		$7.8396e-09$	4.00

Table 26: $L = 10$: Convergence orders of the collocation at two and three equidistant collocation points, as well as of the collocation at two Gaussian points.

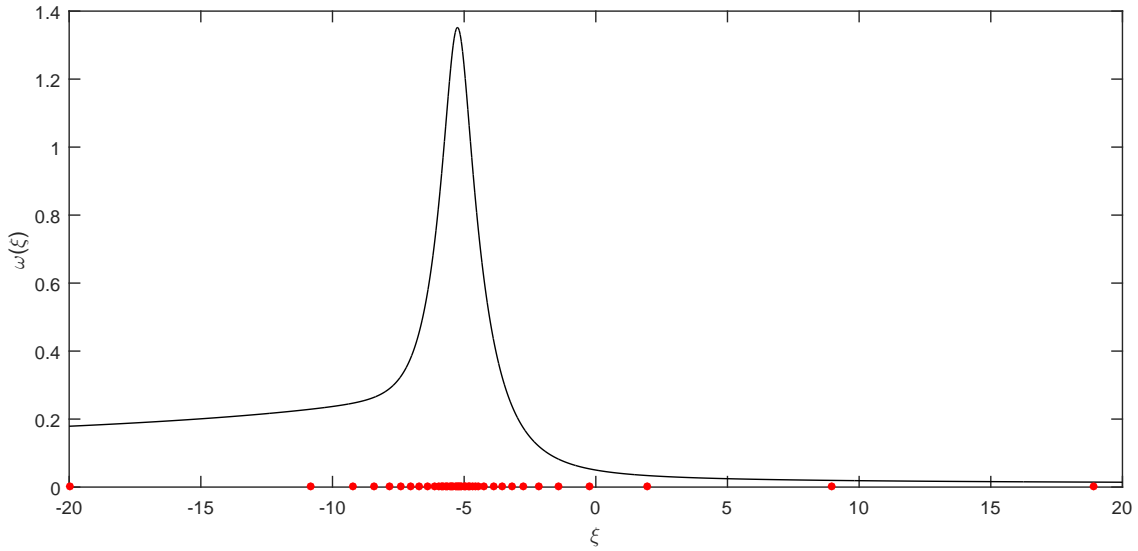
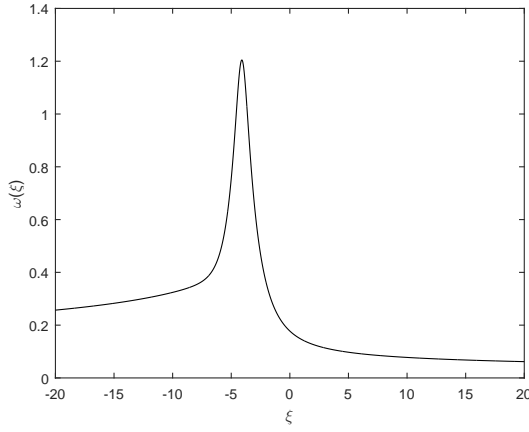


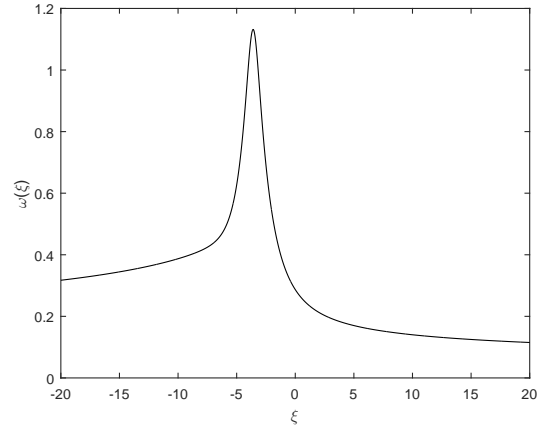
Figure 13: $TOL_a = TOL_r = 10^{-4}$, $M_i = 3200$: Adaptive mesh with 40 out of $M_f = 3332$ subintervals for the collocation at one Gaussian point.

3.3 Solution plots for different values of p

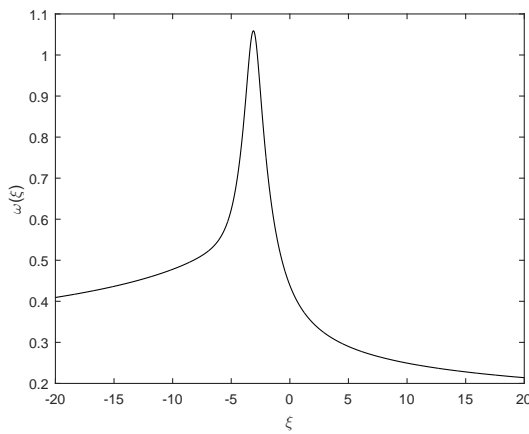
In this section, we plot numerical solutions $w(\xi)$ of the BVP (53)–(55) and $L = 20$ for different values of p . All solutions are changing fast in the central part of the interval of integration $[-20, 20]$.



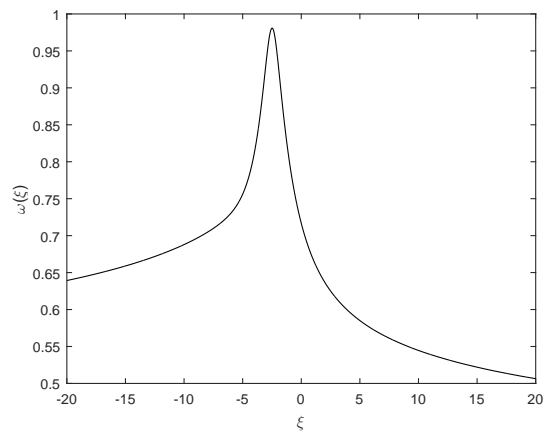
(a) $p = 7$



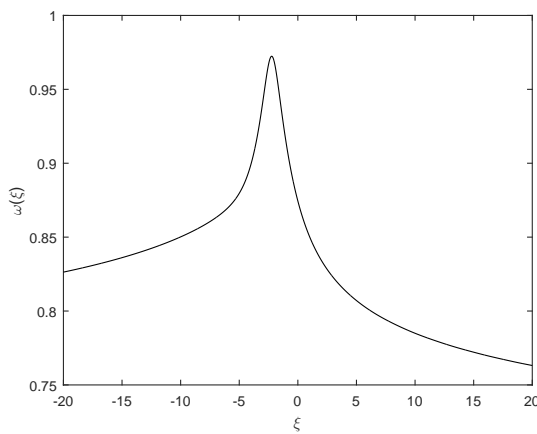
(b) $p = 8$



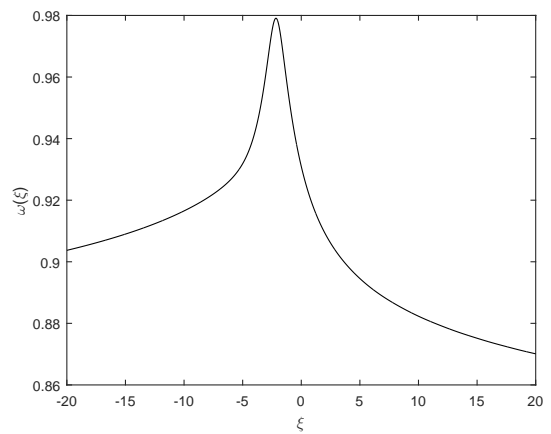
(c) $p = 10$



(d) $p = 20$



(e) $p = 50$



(f) $p = 100$

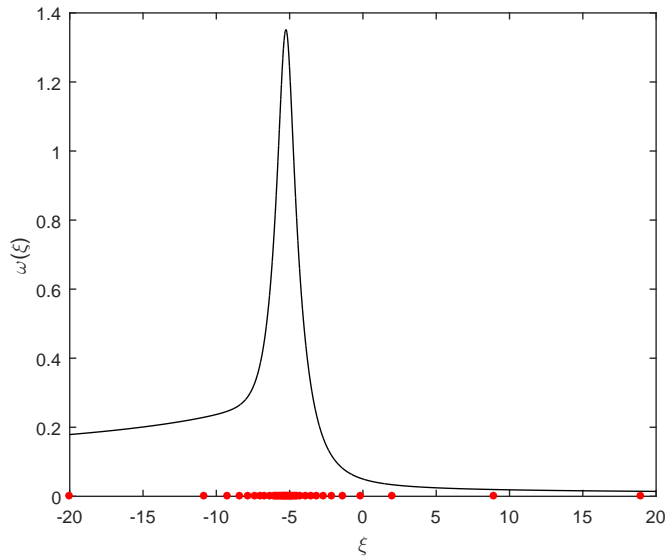
3.4 Solving the problem for $p = 6$ with adaptive mesh option

Here, we solve the problem using the mesh adaptation. For the tolerances $TOL_a = TOL_r = 10^{-4}$, the results can be found in Table 27 and Figure 13. The problem was solved using collocation at one Gaussian point and $L = 20$. M_i is the number of subintervals in the equidistant initial mesh, M_f is the number of subintervals in the final mesh. Figure 13 shows for $M_i = 3200$ a typical location of the mesh points which become denser in the region where the solution changes fast. In the figure, we only show 40 mesh points out of 3333. Typically, the number of mesh points in the final mesh does not depend on M_i in case that M_i is sufficiently large to provide dependable information on the solution structure. If M_i is too large, the code may reduce the number of mesh points. The rather dense mesh is due to the low method order and rough solution behaviour (long interval of integration).

In the next run, we choose two Gaussian collocation points and reduce M_i to $M_i = 100$. Then, we require $M_f = 558$ to satisfy the tolerance with an estimated error of $1.1796e - 05$. If we move to three Gaussian points and start with $M_i = 67$, then the code provides a solution whose estimated error is $3.9856e - 6$ with $M_f = 264$. In the latter cases, the values of $w(-6)$, $w(0)$ and $\|w\|_\infty$ are exactly the same, see below.

M_i	M_f	err_{abs}
200	3332	$1.0189e - 04$
400	3332	$1.0189e - 04$
800	3332	$1.0189e - 04$
1600	3332	$1.0189e - 04$
3200	3332	$1.0189e - 04$

Table 27



$$L = 20 : w(-6) = 0.8054 \quad w(0) = 0.0501 \quad \|w\|_\infty = w(-5.25) = 1.3515.$$

3.5 Time evolution of $u(x, t)$

In the previous computations we obtained the solution $w(\xi)$, $\xi = \frac{x}{(T-t)^{1/3}}$, of the BVP (53)–(55). We now use this result to plot the self-similar blow-up solution of the GKdV equation,

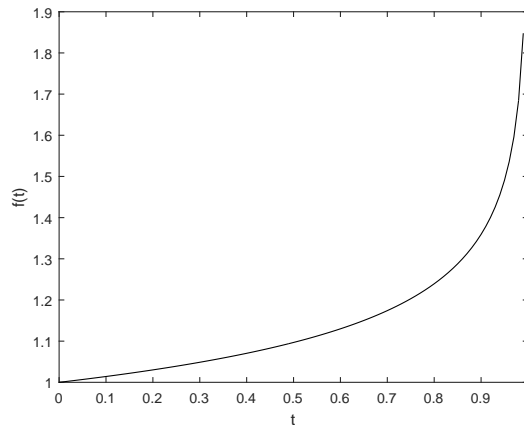
$$u(x, t) = \frac{1}{(T-t)^{2/(3(p-1))}} w\left(\frac{x}{(T-t)^{1/3}}\right),$$

for different values $t \in [0, 1)$, $T = 1$, and $x \in [-20, 20]$. The results are collected in Table 28. In the first column the time distance $1 - t$ from the blow-up point $T = 1$ is shown. In the next column we specify the value of x_{\max} for which $u(x, t)$ becomes maximal. The value of this maximum can be found in the third column. Finally, in the last column, we provide the approximation for the L_2 norm of the solution u .

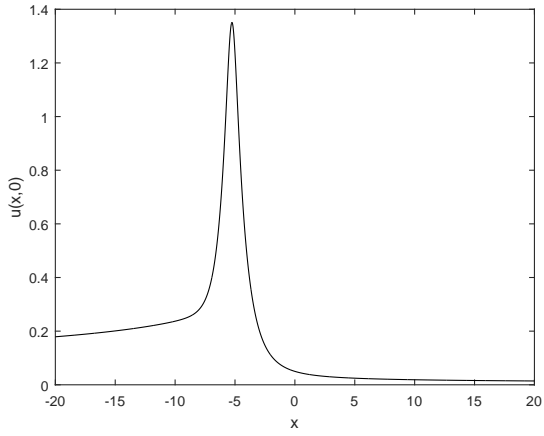
$1 - t$	x_{\max}	$u(x_{\max}, t)$	$\ u(x, t)\ _{L^2}$
10^0	-5.25000	1.3515	3.2210
10^{-3}	-0.52670	3.3914	3.2173
10^{-6}	-0.05260	8.5145	3.2048
10^{-9}	-0.00530	21.3537	3.3902
10^{-12}	-0.00050	53.7897	3.5184
10^{-15}	-0.00005	135.2446	3.6254

Table 28: Characteristic data for $u(x, t)$ as $t \rightarrow 1$.

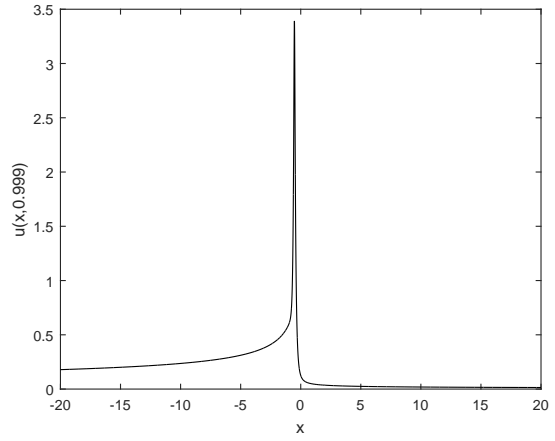
Table 28 clearly indicates a blow-up character of $u(x, t)$ but the maximum of $u(x, t)$ grows slowly. This is due to the slow growth of the factor function $f(t) = \frac{1}{(T-t)^{2/(3(p-1))}}$, $p = 6$, in u .



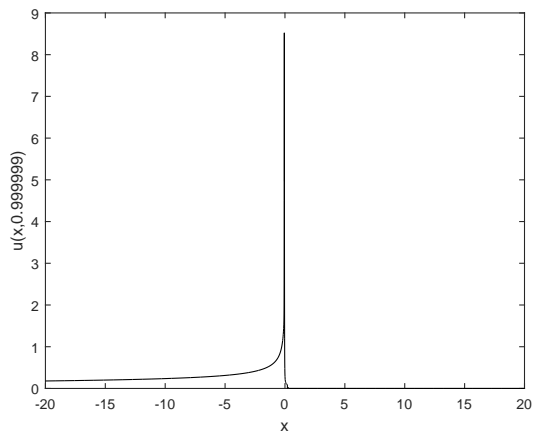
The following plots were calculated using collocation at one Gaussian point.



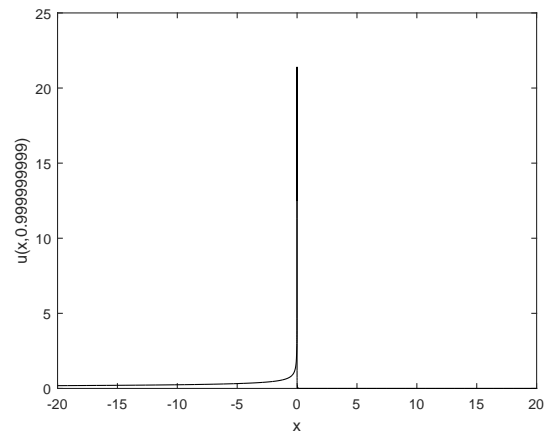
(a) $1 - t = 1$



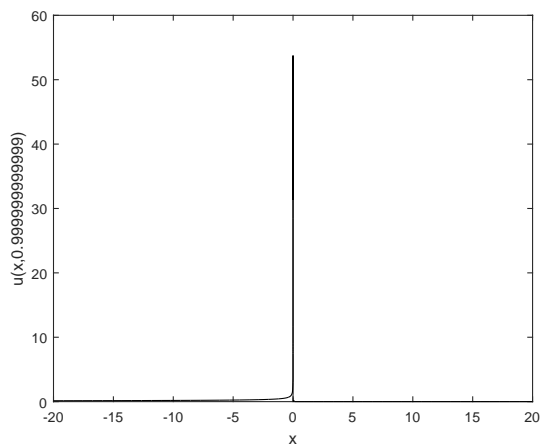
(b) $1 - t = 10^{-3}$



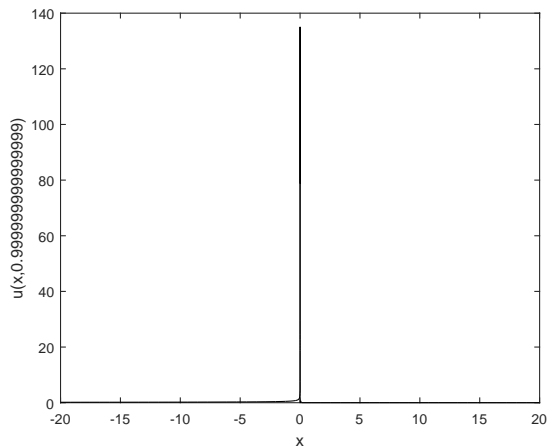
(c) $1 - t = 10^{-6}$



(d) $1 - t = 10^{-9}$



(e) $1 - t = 10^{-12}$



(f) $1 - t = 10^{-15}$

3.6 Reduction of p from $p = 6$ to $p = 5$

Let us consider the BVP (53)–(55). To see what happens when we slowly reduce the values of p from 6 to 5, we use `bvpsuite` to solve (53)–(55) for each p specified in the following plot.

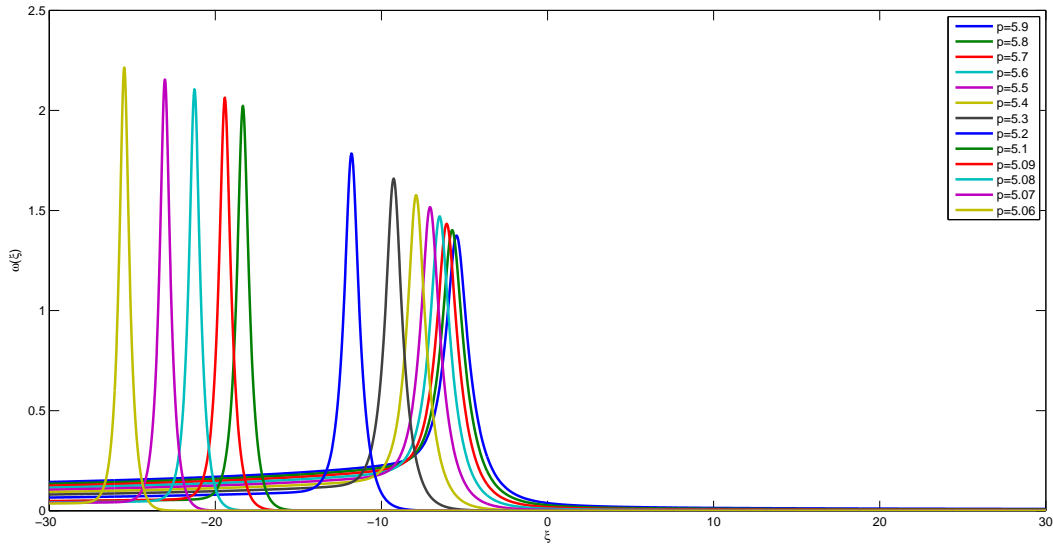


Figure 16: All solutions were calculated using collocation at one Gaussian point.

p	ξ_{\max}	$\omega(\xi_{\max})$	$\ \omega\ _{L^2}^2$	$\ \omega'\ _{L^2}^2$	$\ \omega\ _{H^1}^2$
5.9	-5.4750	1.3750	3.3853	1.5448	4.9301
5.8	-5.7375	1.4022	3.2745	1.6892	4.9637
5.7	-6.0750	1.4339	3.1752	1.8634	5.0386
5.6	-6.4875	1.4713	3.0735	2.0911	5.1646
5.5	-7.0875	1.5168	2.9831	2.3778	5.3609
5.4	-7.9125	1.5773	2.8905	2.8139	5.7044
5.3	-9.2625	1.6597	2.8135	3.4660	6.2795
5.2	-11.8125	1.7846	2.7295	4.6628	7.3923

Table 29: Characteristic data for $\omega(\xi)$ as $p \rightarrow 5$, for $\xi \in [-30, 30]$.

p	ξ_{\max}	$\omega(\xi_{\max})$	$\ \omega\ _{L^2}^2$	$\ \omega'\ _{L^2}^2$	$\ \omega\ _{H^1}^2$
5.1	-18.3375	2.0291	2.6941	7.6880	10.3821
5.09	-19.4875	2.0625	2.6928	8.2956	10.9884
5.08	-21.2625	2.1078	2.6909	9.0208	11.7117
5.07	-23.0437	2.1545	2.6761	9.8819	12.5580
5.06	-25.4812	2.2105	2.6186	10.9553	13.6369

Table 30: Characteristic data for $\omega(\xi)$ as $p \rightarrow 5$, for $\xi \in [-30, 30]$.

p	ξ_{\max}	$\omega(\xi_{\max})$	$\ \omega\ _{L^2}^2$	$\ \omega'\ _{L^2}^2$	$\ \omega\ _{H^1}^2$
5.1	-18.3375	2.0291	2.7091	7.6880	10.3971
5.09	-19.4875	2.0625	2.7069	8.2956	11.0025
5.08	-21.2625	2.1078	2.7042	9.0208	11.7250
5.07	-23.0437	2.1545	2.7028	9.8819	12.5847
5.06	-25.4812	2.2105	2.7015	10.9553	13.6568

Table 31: Characteristic data for $\omega(\xi)$ as $p \rightarrow 5$, for $\xi \in [-40, 40]$.

p	ξ_{\max}	$\omega(\xi_{\max})$	$\ \omega\ _{L^2}^2$	$\ \omega'\ _{L^2}^2$	$\ \omega\ _{H^1}^2$
5.1	-18.3375	2.0291	2.7801	7.6880	10.4681
5.09	-19.4875	2.0625	2.7621	8.2956	11.0577
5.08	-21.2625	2.1078	2.7562	9.0208	11.7770
5.07	-23.0437	2.1545	2.7450	9.8819	12.6269
5.06	-25.4812	2.2105	2.7388	10.9553	13.6941

Table 32: Characteristic data for $\omega(\xi)$ as $p \rightarrow 5$, for $\xi \in [-100, 100]$.

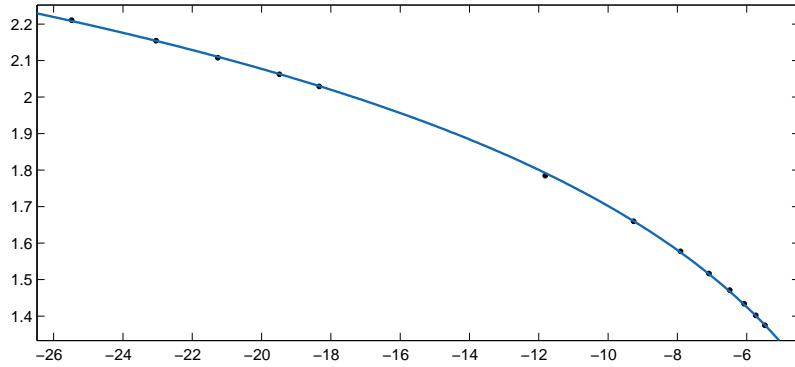


Figure 17: The maxima of the functions $\omega(\xi)$ for different values of p seem to be located on a logarithmic curve.

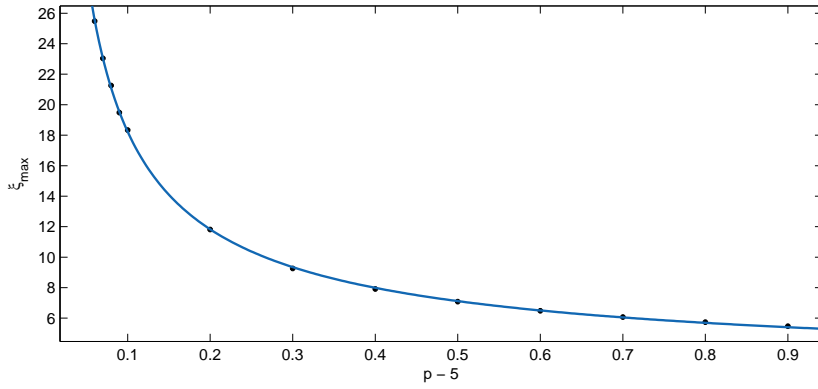
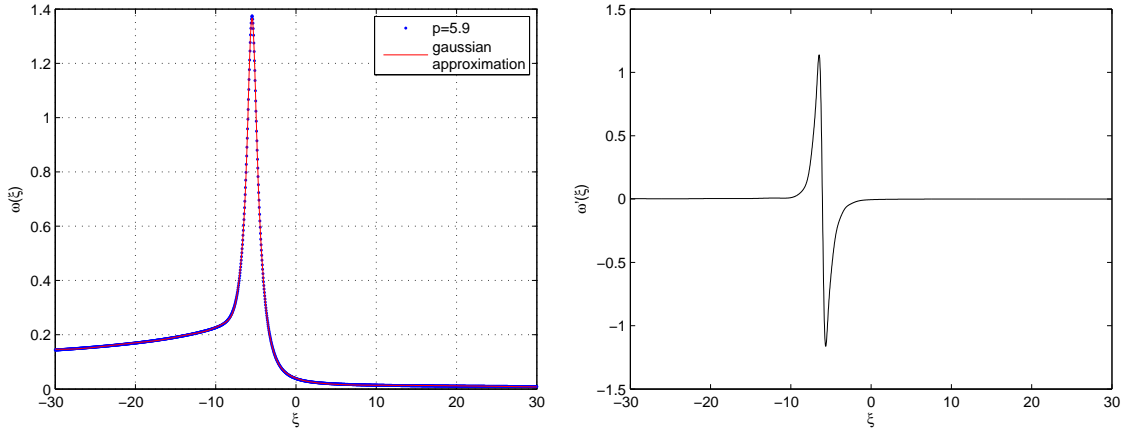


Figure 18: The ξ_{max} - values on a curve of the type $g(x) = a \cdot x^b + c$.

Before calculating the H^1 norm of the above numerical approximation, we approximate them by a sum of at most eight Gaussian functions,

$$\omega(\xi) \approx g(\xi) = \sum_{i=1}^8 a_i \exp \left(- \left(\frac{\xi - b_i}{c_i} \right)^2 \right). \quad (56)$$

To illustrate the quality of the approximation specified in (56), we plot for $\xi \in [-30, 30]$ the numerical values of ω against g in Figure 19A and the approximation for ω' in Figure 19B.



(a) Approximation for $\omega(\xi)$ via $g(\xi)$.

(b) Approximation for $\omega'(\xi)$ via $g'(\xi)$.

Figure 19: $p = 5.9$: Quality of the approximation specified in (56).

3.7 Comparing the self-similar and homoclinic solutions.

We now compare the behaviour close to the peak of the self-similar solutions of the BVP (53)–(55) and the homoclinic solutions of the following BVP, $p = q$ ($5 < q < 6$):

$$Q_{zz} - Q + Q^5 = 0, \quad z \in [a, b], \quad (57)$$

$$Q(a) = Q(b), \quad (58)$$

$$Q_z(a) = Q_z(b), \quad (59)$$

where z is the scaled coordinate, $z = \frac{\xi - \xi^*}{\text{eps}^{1/3}}$ with $\text{eps} = q - 5$ and $\xi^* = -\text{eps}^{-2/3}$.

For the investigation, we use $\xi \in [-30, 30]$, thus it follows that $a = z_{\min} = \frac{-30 - \xi^*}{\text{eps}^{1/3}}$ and $b = z_{\max} = \frac{30 - \xi^*}{\text{eps}^{1/3}}$. Different solutions of the nonlinear BVP (57)–(59) have been obtained using different starting profiles. Figure 20 indicates that the solutions of (57)–(59) move along the z -axis, with a constant width and maximum.

To make a comparison between the homoclinic solution $Q(z)$ of the BVP (57)–(59) and the related solution $\omega(\xi)$ of the BVP (53)–(55) for a given value of $p = q$ ($5 < q < 6$), the appropriate initial profile has to be found such that after the variable transformation, the peak of the homoclinic solution Q is consistent with the peak of the self-similar solution ω which we now denote by $\omega(\xi, p = q)$ to indicate the size of p .

Let us now for $p = 5.2$ describe the procedure step by step. We consider $\omega(\xi)$ for $p = 5.2$, $\omega(\xi, p = 5.2)$. In this case $\text{eps} = 0.2$ and therefore $z \in [-46.2993, 56.2993]$.

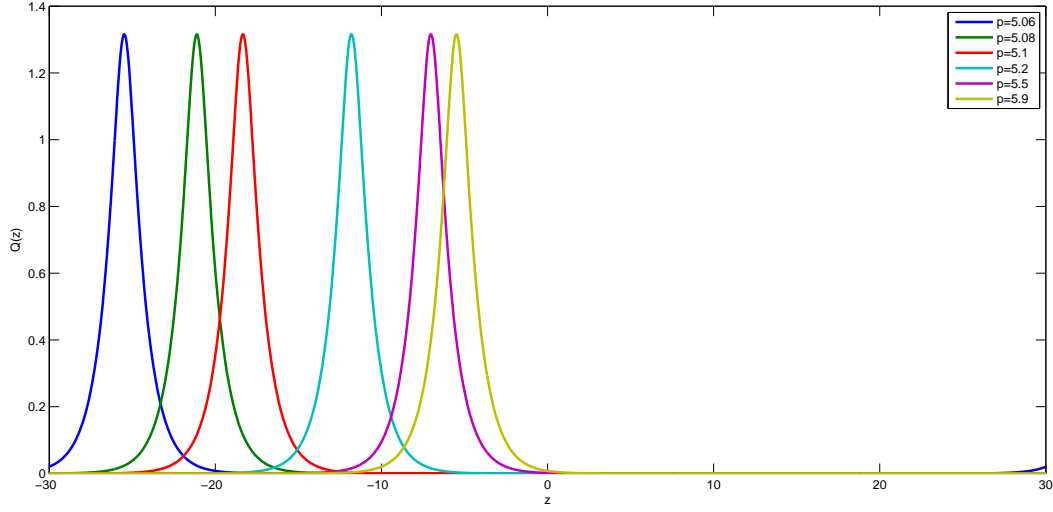
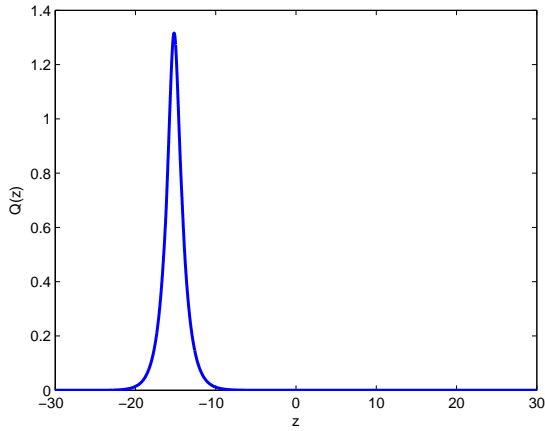


Figure 20: Solutions $Q(z)$, $z \in [-30, 30]$, of the BVP (57)–(59) obtained using with $\omega(\xi)$ as starting profiles.

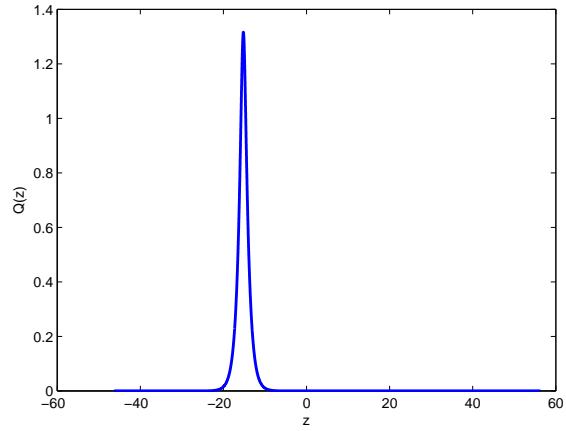
As the initial guess for the solution of (57)–(59) we choose the transformed function $\omega\left(\frac{\xi - \xi^*}{\text{eps}^{1/3}}, p = 5.2\right)$. The respective solution of (57)–(59) is shown in Figure 21b. If we apply the inverse transformation $\xi = z \text{eps}^{1/3} + \xi^*$ to $Q(z)$, then the homoclinic solution $Q(z \text{eps}^{1/3} + \xi^*)$ is scaled to $[-30, 30]$ and can be compared to $\omega(\xi, p = 5.2)$ (see Figure 21c). To align the heights of the maxima and make the homoclinic solution fully comparable to the self-similar one, we multiply $Q(z \cdot \text{eps}^{1/3} + \xi^*)$ by the ratio of the two maxima,

$$Q_a(z \cdot \text{eps}^{1/3} + \xi^*) := \frac{\max(\omega(\xi, p = 5.2))}{\max(Q(z))} \cdot Q(z \cdot \text{eps}^{1/3} + \xi^*). \quad (60)$$

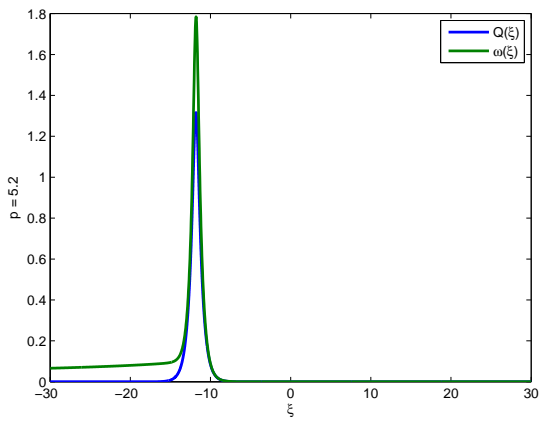
The adapted homoclinic solution Q_a is now very well reflecting the behaviour of the self-similar solution near the peak, see Figure 21d.



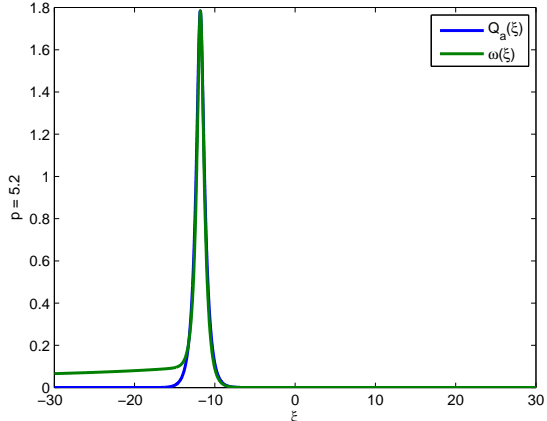
(a) $Q(z)$ with $z \in [-30, 30]$ computed from the initial guess $\omega\left(\frac{\xi - \xi^*}{\text{eps}^{1/3}}, p = 5.2\right)$.



(b) $Q(z)$ with $z \in [-46.2993, 56.2993]$ from the initial guess $\omega\left(\frac{\xi - \xi^*}{\text{eps}^{1/3}}, p = 5.2\right)$.



(c) Comparison between $Q(z \cdot \text{eps}^{1/3} + \xi^*)$ and $\omega(\xi)$.



(d) Comparison between $Q_a(z \cdot \text{eps}^{1/3} + \xi^*)$ and $\omega(\xi)$.

Figure 21: Construction of a homoclinic solution of the BVP (57)–(59) related to the self-similar solution of the BVP (53)–(55) for $p = 5.2$.

The following plots show the homoclinic solutions $Q(z)$ and the self-similar solutions $\omega(\xi)$ for different values of p .

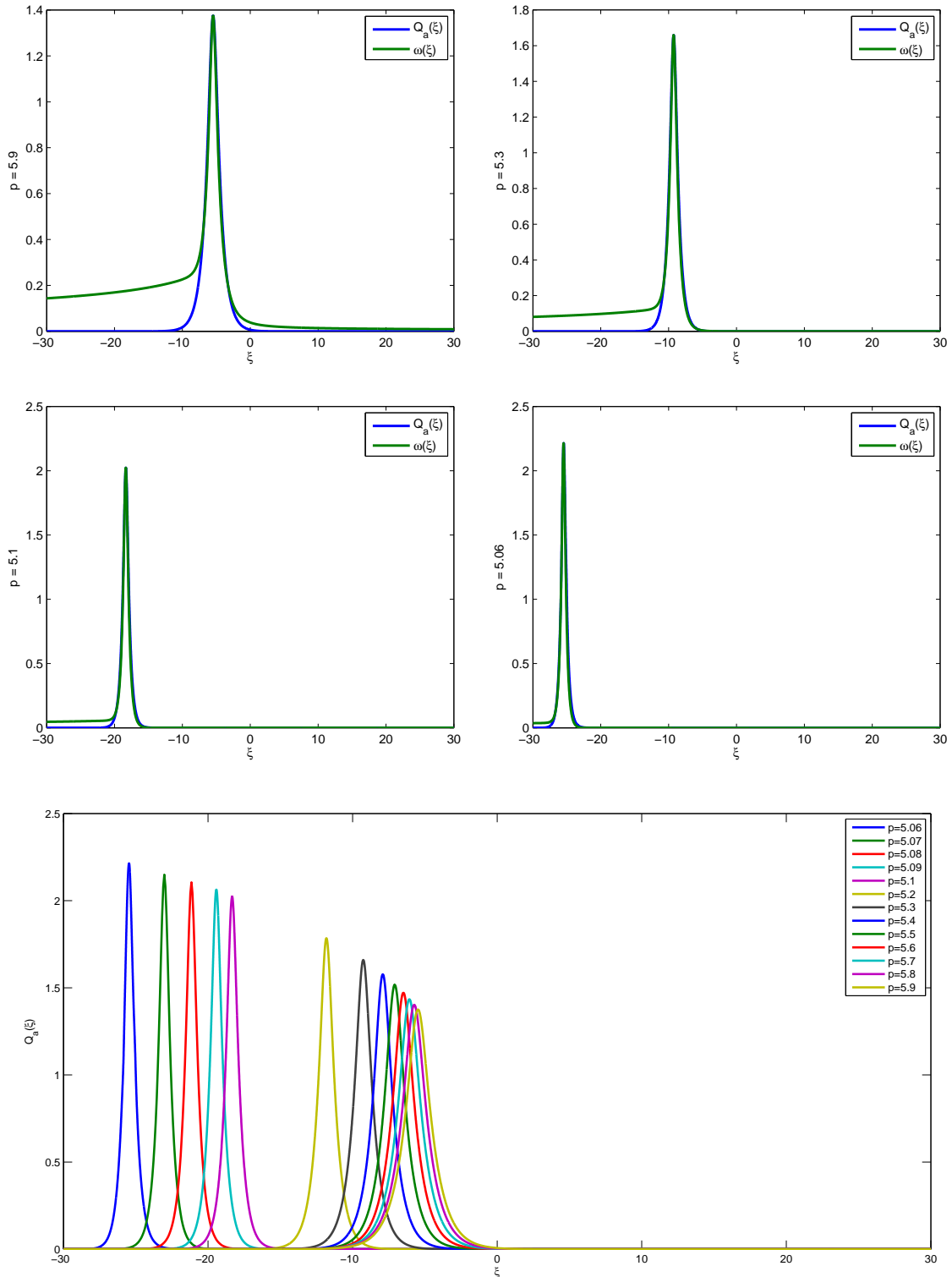


Figure 22: Comparison of $Q_a(\xi)$ and $\omega(\xi)$ for $p \in \{5.9, 5.3, 5.1, 5.06\}$, as well as $Q_a(\xi)$ for all values of p listed in Tables 29 and 30.

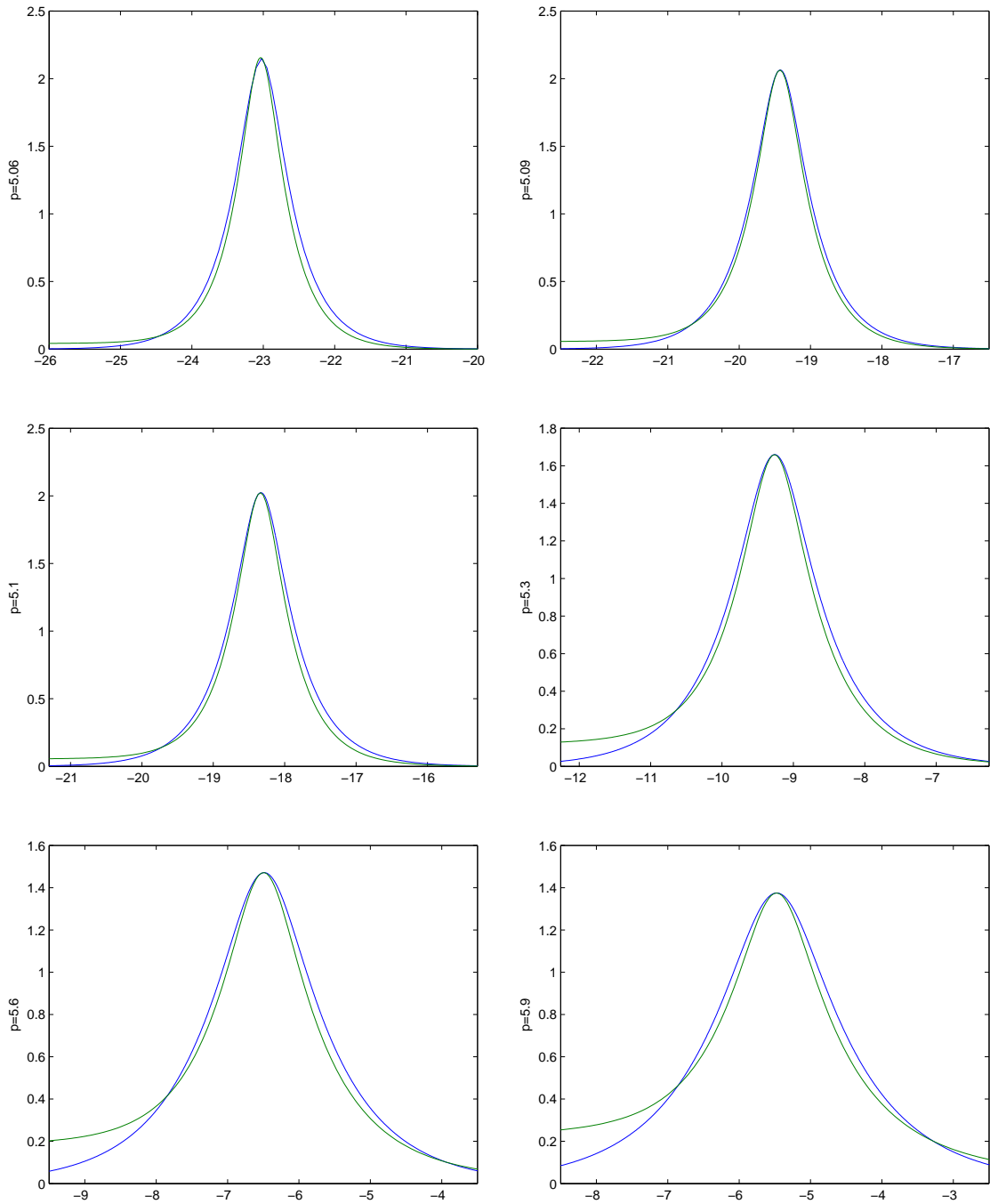


Figure 23: Comparison of Q_a (in blue) and ω (in green) for $p \in \{5.06, 5.09, 5.1, 5.3, 5.6, 5.9\}$.

3.8 Problem Setting ($p = 5$)

In the case of $p = 5$, we consider the following BVP,

$$v_{\xi\xi} - \frac{1}{12}\xi v + \frac{1}{12}v^q = 0, \quad \xi \in \mathbb{R}, \quad (61)$$

$$v(\xi) \xrightarrow{\xi \rightarrow \infty} 0, \quad v(0) = 1, \quad (62)$$

where $q \in \mathbb{N}$, $q \geq 1$. To solve the above problem using `bvpsuite`, we again reduce the domain of ξ to $[-L, L]$, where L is sufficiently large,

$$v_{\xi\xi} - \frac{1}{12}\xi v + \frac{1}{12}v^q = 0, \quad \xi \in (-L, L), \quad (63)$$

$$v(L) = 0, \quad v(0) = 1. \quad (64)$$

Below, we specify the input data for the GUI.

Field	Input value
Orders / Parameters / c	[2] / 0 / [0 L]
Mesh	<code>linspace(-L, L, 10 * L)</code>
Equations	$z1'' - 1/12 * t * z1 + 1/12 * z1^q = 0;$
Boundary / Additional conditions	$z1(c1) = 1;$ $z1(c2) = 0;$
Initial Mesh	<code>linspace(-L,L,10* L)</code>
Initial values	<code>exp(-(linspace(-L,L,10* L)).^2)</code>

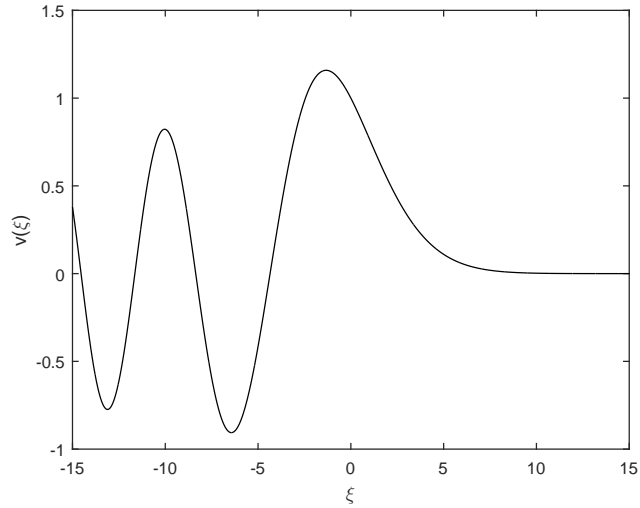
Table 33: Settings for the MATLAB code `bvpsuite` GUI to reproduce the results for selectable q and L .

As previously, in the following tables and figures, we collect the results of the numerical simulations for the BVP (63)–(64). We are especially interested in finding the value of $v'(0)$. We provide this value by interpolating v in the neighbourhood of $\xi = 0$ by a polynomial of degree four and taking its derivative at $\xi = 0$.

3.8.1 Convergence orders and plots of numerical solutions for $p = 5$

$50 \cdot h$	err_{abs}	ord
2^{-0}	$2.3000e - 03$	—
2^{-1}	$5.6831e - 04$	2.00
2^{-2}	$1.4212e - 04$	2.00
2^{-3}	$3.5533e - 05$	2.00
2^{-4}	$8.8835e - 06$	2.00

Table 34: $L = 15$

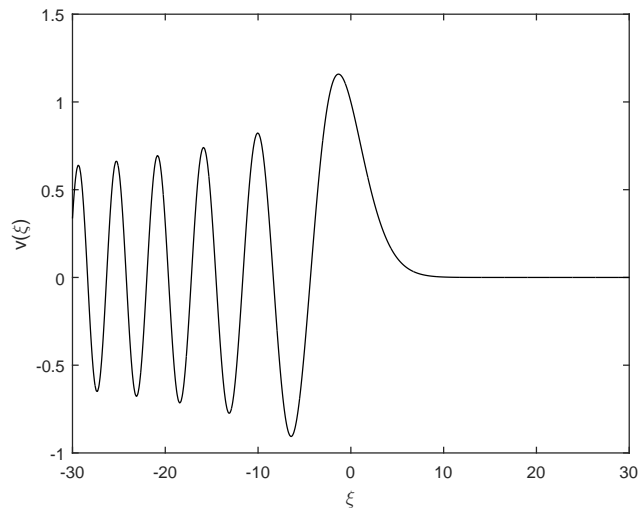


$$L = 15 : v'(0) = -0.2773$$

Table 34 shows the convergence order of the collocation at one Gaussian point for $L = 15$ and $q = 1$.

$50 \cdot h$	err_{abs}	ord
2^{-0}	$9.1000e - 03$	—
2^{-1}	$2.3000e - 03$	2.00
2^{-2}	$5.7097e - 04$	2.00
2^{-3}	$1.4276e - 04$	2.00
2^{-4}	$3.5692e - 05$	2.00

Table 35: $L = 30$

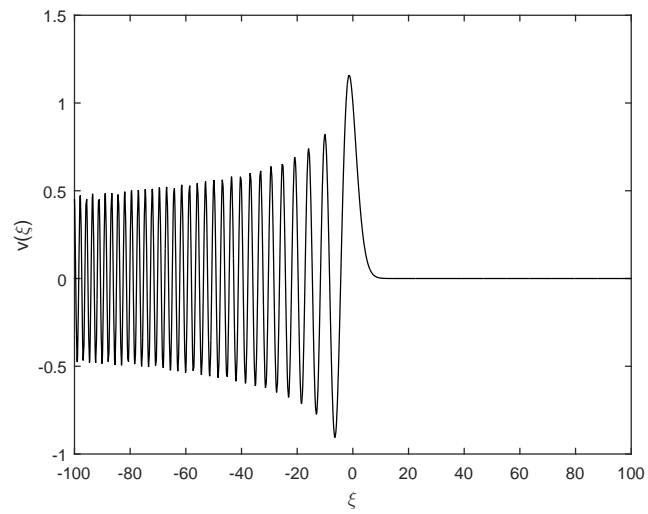


$$L = 30 : v'(0) = -0.2773$$

Table 35 shows the convergence order of the collocation at one Gaussian point for $L = 30$ and $q = 1$.

$50 \cdot h$	err_{abs}	ord
2^{-0}	0.5459	—
2^{-1}	0.1427	1.94
2^{-2}	0.0360	1.97
2^{-3}	0.0090	2.00
2^{-4}	0.0023	2.00

Table 36: $L = 100$

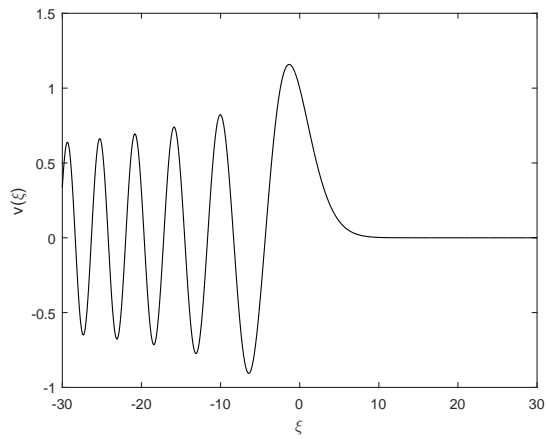


$$L = 100 : v'(0) = -0.2773$$

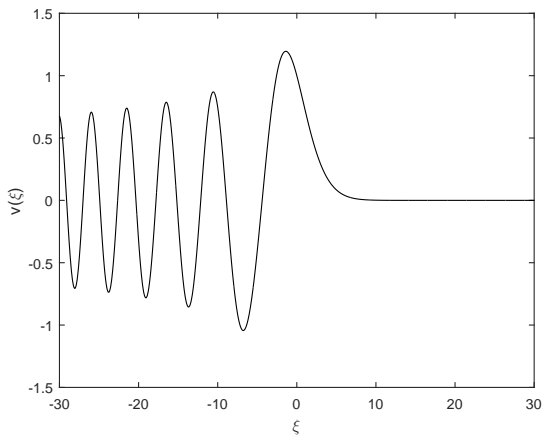
Table 36 shows the convergence order of the collocation at one Gaussian point for $L = 100$ and $q = 1$.

Finally, in the last section, we provide the solution plots for different values of q .

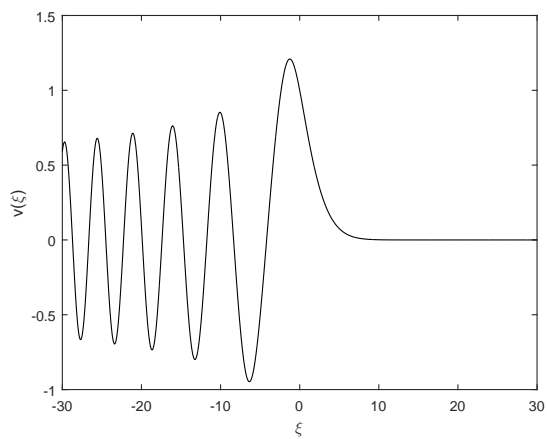
3.8.2 Solution plots for different values of q



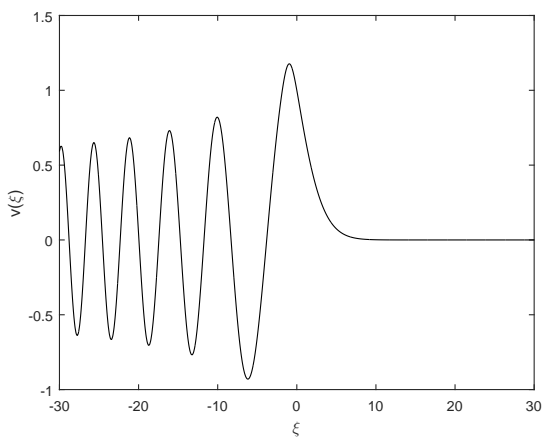
(a) $q = 1$



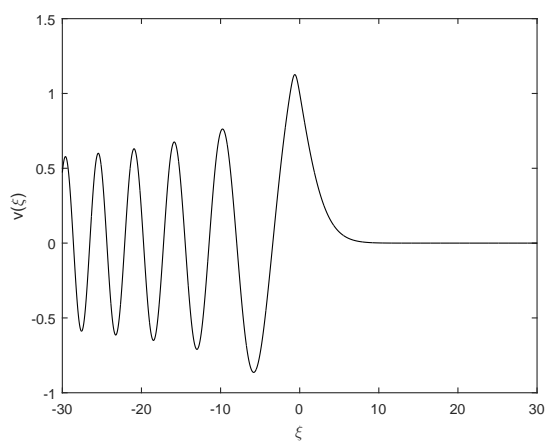
(b) $q = 2$



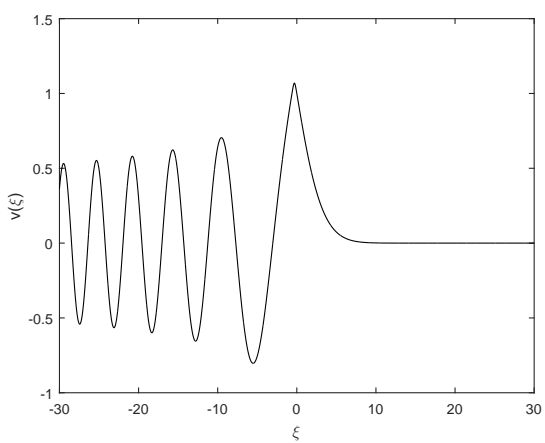
(c) $q = 5$



(d) $q = 10$



(e) $q = 20$



(f) $q = 50$

3.9 Conclusions

The aim of this section has been the computation and further investigation of a solution of the BVP

$$\begin{aligned}\frac{2}{3(p-1)}w + \frac{\xi}{3}w_\xi + (w_{\xi\xi} + w^p)_\xi &= 0, \quad \xi \in \mathbb{R}, \\ \frac{2}{3(p-1)}w(\xi) + \frac{\xi}{3}w_\xi(\xi) &\xrightarrow{\xi \rightarrow \pm\infty} 0, \\ w_{\xi\xi}(\xi) &\xrightarrow{\xi \rightarrow \infty} 0,\end{aligned}$$

by reducing ξ to a finite interval $[-L, L]$ with a sufficiently large L . We have used the open domain MATLAB code `bvpsuite` to solve the problem and have obtained a solution w which changes fast in the central region of the interval of integration. We further have observed classical convergence orders of the collocation scheme with one respectively two Gaussian points and two respectively three equidistant points. Using the adaptive mesh option, a proper location of the mesh points has been observed with higher density of meshpoints in the region where the solution changes fast.

By solving the BVP (57)–(59) in Subsection 3.7, we have found a solution that reflects the behaviour of the self-similar solution near the peak. This result may be used to provide an asymptotic theory for $p \rightarrow 5$. The code `bvpsuite` showed to be reliable and helpful. Especially the options *mesh adaption* and *error estimation* enabled to obtain results in an efficient and fast way. All results from `bvpsuite` support the existing theories.

References

- [1] M.J. ABLOWITZ, M. KRUSKAL AND H. SEGUR, *A note on Miura's transformation*, J. Math. Phys. **20** (1979), 999–1003.
- [2] U. ASCHER AND U. BADER, *A new basis implementation for a mixed order boundary value ODE solver*, SIAM J. Scient. Stat. Comput. **8** (1987), 483–500.
- [3] U. ASCHER, J. CHRISTIANSEN, AND R. RUSSELL, *Collocation software for boundary value ODEs*, ACM Trans. Math. Software **7** (1981), 209–222.
- [4] U. ASCHER, R.M.M. MATTHEIJ, AND R.D. RUSSELL, *Numerical Solution of Boundary Value Problems for Ordinary Differential Equations*, Prentice-Hall, Englewood Cliffs, NJ (1988).
- [5] W. AUZINGER, G. KNEISL, O. KOCH, AND E. WEINMÜLLER, *A Solution Routine for Singular Boundary Value Problems*, Technical Report, ANUM Preprint No., 1/02, Vienna University of Technology, Austria (2002).

- [6] W. AUZINGER, G. KNEISL, O. KOCH, AND E. WEINMÜLLER, *A collocation code for boundary value problems in ordinary differential equations*, Numer. Algorithms **33** (2003), 27–39.
- [7] W. AUZINGER, O. KOCH, D. PRAETORIUS, G. PULVERER, AND E. WEINMÜLLER, *Performance of collocation software for singular BVPs*, ANUM Preprint No. 4/04, Vienna University of Technology, Austria (2004).
- [8] W. AUZINGER, O. KOCH, E. WEINMÜLLER, *Analysis of a New Error Estimate for Collocation Methods Applied to Singular Boundary Value Problems*, SIAM J. Numer. Anal. **42** (2005), 2366–2386.
- [9] W. AUZINGER, O. KOCH, E. WEINMÜLLER, *Efficient Mesh Selection for Collocation Methods Applied to Singular BVPs*, J. Comput. Appl. Math. 1 **180** (2005), 213–227.
- [10] W. AUZINGER, *Numerical Solution of Ordinary Differential Equation*, Lecture Notes, Vienna University of Technology, Vienna, Austria (2003).
- [11] P. BAILEY, W. EVERITT, AND A. ZETTL, *Computing eigenvalues of singular Sturm-Liouville problems*, Results Math. **20** (1991), 391–423.
- [12] G. BADER AND U. ASCHER, *A new basis implementation for a mixed order boundary value ODE solver*, SIAM J. Scient. Stat. Comp. **8** (1987), 483–500.
- [13] M.L. BENJAMIN, *Lectures on nonlinear wave motion*, Lectures in Appl. Math. **15** (1974).
- [14] M.L. BENJAMIN, J.L. BONA AND J.J. MAHONEY, *Model equations for long wave nonlinear dispersive media*, Phil. Trans. R. Soc. Lond. **272** (1971), 47–78.
- [15] J.L. BONA, V.A. DOUGALIS, O.A. KARAKASHIAN AND W.R. MCKINNEY, *Conservative, High-Order Numerical Schemes for the Generalized Korteweg-de Vries Equation*, Phil. Trans. R. Soc. Lond. **351** (1995), 107–164.
- [16] C. BUDD AND R. KUSKE, *Localised periodic pattern for the non-symmetric generalized Swift-Hohenberg equations*, Physica D **208** (2005), 73–95.
- [17] C. BUDD AND J. WILLIAMS, *Parabolic monge-ampère methods for blow-up problems in several spatial dimensions*, J. Phys. A: Math. Gen. **39** (2006), 5425–5463.
- [18] H. CHEN, *Analysis of blow-up for a nonlinear degenerate parabolic equation*, J. Math. Anal. Appl. **192** (1995), 180–193.
- [19] H. CHEN, *On a singular nonlinear elliptic equation*, Nonlin. Anal., TMA **29** (1997), 337–345.

- [20] D.B. DIX AND W.R. MCKINNEY, *Numerical computations of self-similar blow-up solutions of the generalized Korteweg-de Vries equation*, *Differential Integral Equations* **11** (1998), 679–723.
- [21] M. DRMOTA, R. SCHEIDL, H. TROGER, AND E. WEINMÜLLER, *On the imperfection sensitivity of complete spherical shells*, *Comp. Mech.*, **2** (1987), 63–74.
- [22] G. FROMENT AND K. BISCHOFF, *Chemical reactor analysis and design*, John Wiley & Sons Inc., New York (1990).
- [23] F. FROMMLET AND E. WEINMÜLLER, *Asymptotic error expansions for singular boundary value problems*, *Math. Models Methods Appl. Sci.* **11** (2001), 71–85.
- [24] F. GAZZOLA, J. SERRIN AND M. TANG, *Existence of ground states and free boundary problems for quasilinear elliptic operators*, *Adv. Differential Equations* **5** (1-3) (2000), 1–30.
- [25] S. GOLUB, *Measures of restrictions in inward foreign direct investment in OECD countries*, OECD Economics Dept. WP Nr. 357.
- [26] G.HASTERMANN, P.M. LIMA, M.L. MORGADO, AND E. WEINMÜLLER, *Numerical solution of the density profile equation with p -Laplacians*, Vienna Technical University, ASC Report No. 43/2011, available at <http://www.asc.tuwien.ac.at/preprint/2011/asc43X2011.pdf>.
- [27] E. HELPMAN, M. MELITZ, AND YEAPLE, *Export versus FDI with heterogeneous firms*, *Amer. Econ. Rev.* **94** (2004), 300–316.
- [28] F. D. HOOG AND R. WEISS, *The application of Runge-Kutta schemes to singular initial value problems*, *Math. Comp.* **44** (1985), 93–103.
- [29] F. D. HOOG AND R. WEISS, *Collocation methods for singular boundary value problems*, *SIAM J. Numer. Anal.* **15** (1978), 198–217.
- [30] B. KARABAY, *Foreign direct investment and host country policies: A rationale for using ownership restrictions*, tech. report, University of Virginia, WP (2005).
- [31] T. KAPITULA, *Existence and stability of singular heteroclinic orbits for the Ginzburg-Landau equation*, *Nonlinearity* **9** (1996), 669–685.
- [32] H.B. KELLER, *Approximation Methods for Nonlinear Problems with Application to Two-Point Boundary Value Problems*, *Math. Comp.* **29** (1975), 464–474.
- [33] H.B. KELLER, *Accurate difference methods for nonlinear two point boundary value problems*, *SIAM J. Numer. Anal.* **11** (1974), 305–320.

- [34] G. KITZHOFFER, O. KOCH, P. LIMA, AND E. WEINMÜLLER, *Efficient Numerical Solution of the Density Profile Equation in Hydrodynamics* J. Sci. Comput. **32** (2007), 411–424.
- [35] G. KITZHOFFER, O. KOCH, AND E. WEINMÜLLER, *Pathfollowing for essentially singular boundary value problems with application to the complex Ginzburg–Landau equation*, BIT **49** (2009), 141–160.
- [36] G. KITZHOFFER, O. KOCH, G. PULVERER, CH. SIMON, AND E. WEINMÜLLER, *The new Matlab code bvpsuite for the solution of singular implicit BVPs*, J. Numer. Anal. Indust. Appl. Math. **5** (2010), 113–134.
- [37] O. KOCH AND E. WEINMÜLLER, *Analytical and Numerical Treatment of a Singular Initial Value Problem in Avalanche Modeling*, Appl. Math. and Comput. **148** (2004), 561–570.
- [38] O. KOCH, *Asymptotically correct error estimation for collocation methods applied to singular boundary value problems*, Numer. Math. (2005), 143–164.
- [39] D.J. KORTEWEG AND G. DE VRIES, *On the change of form of long waves advancing in a rectangular canal, and on a new type of long stationary waves*, Philos. Mag. **5** (1895), 422–443.
- [40] E. KREYSZIG, *Introductory Functional Analysis with Applications*, SIAM Rev. **21** (1979), 412–413.
- [41] P.D. LAX, *Integrals of nonlinear equations of evolution and solitary waves*, Comm. Pure. Appl. Math. **21** (1968), 467–490.
- [42] P.M. LIMA AND M. L. MORGADO, *Efficient computational methods for singular free boundary problems using smoothing variable substitutions*, J. Comput. Appl. Math. **236** (2012), 2981–2989.
- [43] D.M. MCCLUNG AND A.I. MEARS, *Dry-flowing avalanche run-up and run-out*, J. Glaciol. **41** (1995), 359–369.
- [44] R.M. MIURA, *The Korteweg-de Vries equation: A survey of results*, SIAM Rev. **18** (1976), 412–459.
- [45] G. MOORE, *Geometric methods for computing invariant manifolds*, Appl. Numer. Math. **17** (1995), 319–331.
- [46] M.L. MORGADO AND P.M. LIMA, *Numerical solution of a class of singular free boundary problems involving the m -Laplace operator*, J. Comput. Appl. Math. **234** (2010), 2838–2847.

- [47] R. MÄRZ AND E. WEINMÜLLER, *Solvability of boundary value problems for systems of singular differential-algebraic equations*, SIAM J. Math. Anal. **24** (1993), 200–215.
- [48] J.M. ORTEGA AND W.C. RHEINBOLDT, *Iterative Solution of Nonlinear Equations in Several Variables*, Academic Press, New York (1957).
- [49] G. PULVERER, G. SÖDERLIND, AND E. WEINMÜLLER, *Automatic grid control in adaptive BVP solvers*, Numer. Algorithms **56** (2011), 61–92.
- [50] V. RANADE, *Computational flow modeling for chemical engineering*, Academic Press, San Diego (2002).
- [51] V. ROTTSCHÄFER, C. MEERMAN, AND P. ZEGELING, *Blowup solutions of the Korteweg-de Vries equation*, (2013).
- [52] R.D. RUSSELL AND J. CHRISTIANSEN, *Adaptive mesh selection strategies for solving boundary value problems*, SIAM J. Numer. Anal. **15** (1978), 59–80.
- [53] L. SHAMPINE, J. KIERZENKA, AND M. REICHELT, *Solving Boundary Value Problems for Ordinary Differential Equations in MATLAB with bvp4c* (2000).
- [54] L. SHAMPINE, P. MUIR, AND H. XU, *A user-friendly Fortran BVP solver*, J. Numer. Anal. Indust. Appl. Math., **1** (2006), 201–217.
- [55] A. SPIELAUER, AND E. WEINMÜLLER, *Numerical solution of boundary value problems in ordinary differential equations with time and space singularities*, Vienna Technical University, ASC Report, (2015).
- [56] K. SUNDMACHER AND U. HOFFMANN, *Multicomponent mass and energy transport on different length scales in a packed reactive distillation column for heterogeneously catalyzed fuel ether production*, Chem. Eng. Sci. **49** (1994), 4443–4464.
- [57] E. WEINMÜLLER, *Collocation for singular boundary value problems of second order*, SIAM J. Numer. Anal. **23** (1986), 1062–1095.
- [58] E. WEINMÜLLER AND R. WINKLER, *Path-following algorithm for singular boundary value problems*, ZAMM Z. Angew. Math. Mech. **68** (1988), 527–537.
- [59] R. WINKLER, *Path-following for two-point boundary value problems*, Tech. Rept. 78, Department of Mathematics, Humboldt-University Berlin, Germany (1985).
- [60] C.Y. YEH, A.B. CHEN, D. NICHOLSON, AND W. BUTLER, *Full-potential Korrington-Kohn-Rostoker band theory applied to the Mathieu potential*, Phys. Rev. B **42** (1990), 10976–10982.

- [61] N.J. ZABUSKY, *Fermi-Pasta-Ulam, solitons and the fabric of nonlinear and computational science: History, synergetics, and visiometrics*, *Chaos* **15** (2005).